

# 1 **Reconstructing the ocean's mesopelagic zone** 2 **carbon budget: sensitivity and estimation of** 3 **parameters associated with prokaryotic** 4 **remineralization**

5 Chloé Baumas<sup>1\*#</sup>, Robin Fuchs<sup>1,2\*</sup>, Marc Garel<sup>1</sup>, Jean-Christophe Poggiale<sup>1</sup>, Laurent Memery<sup>3</sup>,  
6 Frédéric A.C. Le Moigne<sup>1,3</sup>, Christian Tamburini<sup>1</sup>

7 *\*Both authors contributed equally*

8 <sup>1</sup>Aix Marseille Univ, Université de Toulon, CNRS, IRD, MIO UM 110, Marseille, France

9 <sup>2</sup>Aix Marseille Univ, CNRS, I2M, Marseille, France

10 <sup>3</sup>LEMAR Laboratoire des Sciences de l'Environnement Marin, UMR6539, CNRS, UBO, IFREMER, IRD, Plouzané,  
11 Technopôle Brest-Iroise, France

12  
13 #Corresponding author : [cbaumas@stanford.edu](mailto:cbaumas@stanford.edu)

## 14 **Abstract**

15 Through the constant rain of sinking marine particles in the ocean, carbon (C) trapped within  
16 is exported into the water column and sequestered when reaching depths below the  
17 mesopelagic zone. Atmospheric CO<sub>2</sub> levels are thereby strongly related to the magnitude of  
18 carbon export fluxes in the mesopelagic zone. Sinking particles represent the main source of  
19 carbon and energy for mesopelagic organisms, attenuating the C export flux along the water  
20 column. Attempts to quantify the amount of C exported versus consumed by heterotrophic  
21 organisms have increased in recent decades. Yet, most of the conducted estimations have led  
22 to estimated C demands several times higher than the measured C export fluxes. The choice  
23 of parameters such as growth efficiencies or various conversion factors is known to greatly  
24 impact the resulting C budget. In parallel, field or experimental data are sorely lacking to  
25 obtain accurate values of these crucial overlooked parameters. In this study, we identify the  
26 most influential of these parameters and perform inversion of a mechanistic model. Further,  
27 we determine the optimal parameter values as the ones that best explain the observed  
28 prokaryotic respiration, ~~the~~ prokaryotic production, and ~~the~~ zooplankton respirations. The  
29 consistency of the resulting C-budget suggests that such budgets can be adequately balanced  
30 when using appropriate parameters.

31 **Keywords:** Biological carbon pump, Optimization methods, Carbon budget, Mesopelagic  
32 zone, prokaryotic carbon demand, model inversion  
33  
34

## 35 1. Introduction

36 The biological carbon pump (BCP) is the main mechanism by which CO<sub>2</sub> is exported and stored  
37 in the deep ocean in the long term. This ecosystem service is defined as the sum of the  
38 biological processes that lead to carbon export from the euphotic zone into the deep ocean  
39 (Eppley and Peterson 1979). This process exports from 5 to 20 Gt C yr<sup>-1</sup> in the form of  
40 particulate organic carbon (POC) gravitationally sinking from the sunlit ocean to the  
41 mesopelagic zone typically located between 200 and 1000 m (Henson et al. 2011). Therefore,  
42 atmospheric CO<sub>2</sub> levels are strongly related to any change in carbon export into the  
43 mesopelagic zone (Kwon et al. 2009). Five downward pathways of organic matter export to  
44 the mesopelagic zone are defined: through phytoplankton (senescent cells, colonies, spores,  
45 cysts), zooplankton (carcasses or fecal pellets), aggregates (marine snow of different  
46 compositions including the two latter categories), vertical migration of zooplankton and  
47 mixing/diffusion/advection (Siegel et al. 2016; Le Moigne 2019).

48 Gravitational sinking POC supply, combining the 3 first pathways described above, constitutes  
49 the main organic carbon input to the mesopelagic zone (Boyd et al. 2019). Consequently, the  
50 downward flux of organic carbon is attenuated with increasing depth as it is fragmented,  
51 metabolized and remineralized by different biological processes until only the refractory  
52 material remains. The majority of POC flux attenuation occurs in the mesopelagic zone (Martin  
53 et al. 1987; Marsay et al. 2015; Fuchs et al. 2022). The remineralization of exported carbon is  
54 mainly performed by two types of organisms: microorganisms (mostly heterotrophic  
55 prokaryotes i.e. Bacteria and Archaea) and zooplankton. Heterotrophic prokaryotes primarily  
56 use dissolved organic carbon (DOC) as a source of carbon. However, some prokaryotes,  
57 colonizing particles upon formation, undergo changes in environmental conditions during their  
58 descent, such as the increase of the hydrostatic pressure and the variations of temperature  
59 (Tamburini et al. 2003, 2021; Baumas et al. 2021). Such particle-attached prokaryotes  
60 primarily use POC as a carbon source. Only organic matter of size below 600 Da diffuses  
61 directly through prokaryotic membranes, therefore attached prokaryotes produce ectoenzymes  
62 required to solubilize larger molecules (Weiss et al. 1991). Smith et al. (1992) observed that  
63 the amount of DOC produced by ectoenzymatic solubilization of POC may be 10 to 100 times  
64 greater than the absorption capacity of a cell. DOC is thereby released into the surrounding

65 water (the so-called solubilization). This increases the amount of DOC available for free-living  
66 prokaryotes. In addition, several types of zooplankton are involved in marine particles: POC-  
67 feeding detritivores (e.g. copepods), prokaryotes consumers (e.g. flagellates), and carnivores  
68 (e.g. chaetognaths). Besides, zooplankton lose POC through excretion (moult, mucilage, urine),  
69 fecal pellets (decomposed organic matter), and sloppy feeding. Giering et al. (2014) specify  
70 that 30% of a particle supplied by the downward flux is fragmented by the action of the  
71 detritivores and is transformed into suspended matter.

72 Given their importance regarding the BCP, all the processes described above were extensively  
73 studied in the last decades (e.g. Alldredge and Silver 1988; Smith et al. 1992; Kiørboe et al.  
74 2002, 2003; Kiørboe 2003; Lampitt et al. 2008; Steinberg et al. 2008; Iversen et al. 2010;  
75 Giering et al. 2014; Koski et al. 2020 and references therein). However, the scientific  
76 community has struggled to reconcile the mesopelagic carbon budget with measurements and  
77 estimates showing a biological carbon demand often greater than the amount of known organic  
78 carbon sources (Reinthal et al. 2006; Steinberg et al. 2008; Burd et al. 2010; Collins et al.  
79 2015; Boyd et al. 2019). In other words, the measured export flux cannot sustain measured  
80 metabolic demands of prokaryotes and zooplankton altogether in the mesopelagic zone, leading  
81 to a discrepancy in C budgets.

82 A first explanation may lie in the choices of the boundaries of the mesopelagic zone used to  
83 integrate fluxes and to estimate the carbon budget as investigated in Fuchs et al. (2022). **Indeed**  
84 **they specifically designed a method to determine from CTD-cast variables (fluorescence, O<sub>2</sub>**  
85 **concentration, potential temperature, salinity, and density) accurate boundaries which vary in**  
86 **space and time.** With their method named RUBALIZ, they show that 90% of the POC flux  
87 attenuation occurs within new determined boundaries which is not the case of the fixed 200-  
88 1000m often used. Besides, integrating prokaryotic C demand within RUBALIZ boundaries  
89 helps to reduce the discrepancy. **Other sources of discrepancy** may be found focusing on the  
90 carbon demand of prokaryotes (which are responsible for the final step of the remineralization),  
91 whose estimation is usually provided by adding rates of prokaryotic heterotrophic production  
92 (PHP) to that of prokaryotic respiration (PR) (Burd et al. 2010). PHP rates are often measured  
93 from tritiated leucine incorporation rates in incubations which are then multiplied by a  
94 conversion factor Leu/Carbon (CF) (Kirchman et al. 1985). The PR is more challenging to  
95 measure (especially in the dark ocean, (Nagata et al. 2010) and, therefore, often estimated from  
96 measurements of PHP and a prokaryotic growth efficiency (PGE) taken from the literature (as  
97  $PR = PHP \times (1-PGE)/PGE$ , del Giorgio and Cole 1998). Unfortunately, *in-situ* measurements

98 of both CF and PGE are time-consuming and operationally complex to perform (especially for  
99 the mesopelagic zone). In addition, such data for **particle-attached prokaryotic communities** are  
100 scarce since the adequate sampling devices (to specifically sample biologically intact sinking  
101 particles) were only recently validated (Baumas et al. 2021). Besides, PHP and PR data are  
102 usually obtained after decompression or carried out from experiments at atmospheric pressure,  
103 being a source of misvaluation (Tamburini et al. 2013). As a result, **mean values from** global  
104 literature compilation or theoretical values are often used as references for both CF or PGE  
105 (Burd et al. 2010; Giering and Evans 2022) and may be far from the actual *in situ* values.

106 In parallel, model predictions help to estimate unmeasurable processes along with the  
107 comparison and validation of data. The biological processes occurring in the mesopelagic zone  
108 are not yet well constrained (see sections above). Consequently, only a few models specifically  
109 designed to assess the fluxes governing the BCP in the mesopelagic zone exist (e.g. Tian et al.  
110 2000; Anderson and Ryabchenko 2009; Anderson and Tang 2010; Fennel et al. 2022). For  
111 instance, the model developed by Anderson and Tang (2010) enables the evaluation of the  
112 remineralization of different compartments such as **particle-attached prokaryotes** to sinking and  
113 suspended particles, free-living prokaryotes and up to six trophic levels of zooplankton. This  
114 model describes the various known biological processes involved in the BCP system. However,  
115 the model also requires to be set up with parameters such as the PGE. For example, Anderson's  
116 model requires **20** parameters which often present large uncertainties.

117 Giering et al. (2014) attempted to reconcile carbon input and biological carbon demand in the  
118 mesopelagic zone using the Anderson and Tang (2010) model and measurements carried out  
119 in the North Atlantic (Porcupine Abyssal Plain site, 49.0°N 16.5°W, summer 2009). They  
120 found that prokaryotes were responsible for 70-92% of the remineralization of organic carbon.  
121 In this study, the model results were consistent with the measurements performed *in situ*, both  
122 showing a reconciliation of the carbon budget between 50 and 1000 m depths. Giering et al.  
123 (2014) balanced their C-budget by using a rather low CF ( $CF = 0.44 \text{ kg C mol}^{-1}$ ) compared to  
124 the one generally used in the literature ( $CF = 1.55 \text{ kg C mol}^{-1}$ ) and a PGE of 8% for free-living  
125 prokaryotes and 24% for **particle-attached prokaryotes**. All these values were chosen as  
126 medians of literature values compiled from various measurement methods. Wisely choosing  
127 these parameter is therefore crucial to determine the reconciliation or the imbalance of carbon  
128 budget.

129 In this respect, we rely on model inversion methods (Tarantola 2005) to provide meaningful  
130 estimations of parameters of interest. For a given phenomenon, inversion methods rely on a

131 model taking as input the parameters to be estimated and whose outputs can be compared with  
132 *in situ* measurements. The inversion procedure thus gives the value of the parameters that best  
133 replicate the *in situ* measurements. This type of procedure has already been used in  
134 oceanography modeling. For instance, Saint-Béat et al. (2018) studied phytoplankton marine  
135 food web in the Arctic and Saint-Béat et al. (2020) examined pelagic ecosystems of two  
136 different zones in the Arctic Baffin Bay using inversion method and sensitivity analyses to  
137 identify which biological processes impact the most the planktonic ecosystem functioning.

138 Here, we investigate the impact of **widely but inadequately used** parameters associated with  
139 the prokaryotic remineralization (e.g. CF, PGEs) on the magnitude of the discrepancy. Our  
140 aims are: 1) to highlight the most sensitive parameters for which the determination of an  
141 accurate value is critical in the context of balancing **the** mesopelagic carbon budget; 2) to  
142 perform a mathematical inversion method to estimate the most plausible *in situ* values of the  
143 most sensitive parameters from a limited field dataset; 3) to discuss our results in the context  
144 of mesopelagic carbon budget **and carbon sequestration by the BCP.**

## 145 **2. Material & methods**

### 146 **2.1 *In situ* Data**

147 Most of the data used in this study originated from the DY032 (June-July 2015) cruise at the  
148 PAP (Porcupine Abyssal Plain) site in the North Atlantic onboard the RRS Discovery. Some  
149 data unavailable for DY032 were estimated from a previous PAP cruise, D341 (July-August  
150 2009). Most of the *in situ* data were compiled from already published cruise data (e.g. Giering  
151 et al. 2014; Belcher et al. 2016; Baumas et al. 2021; Fuchs et al. 2022). Their post-treatments  
152 to suit our study framework are described below. Additionally, we used data (ectoenzymatic  
153 activities along with total hydrolysable amino acids and carbohydrates, depth profile of  
154 heterotrophic prokaryotic production and respiration under *in situ* pressure versus atmospheric)  
155 from the PEACETIME cruise (Guieu et al. 2020) that occurred in May 2017 in the  
156 Mediterranean Sea to illustrate some points in our discussions (see supp data).

#### 157 **2.1.1 Carbon fluxes**

##### 158 **a) Determination of the Active Mesopelagic zone boundaries**

159 Fuchs et al. (2022) introduced the “RUBALIZ” method, using CTD data, which allows the  
160 estimation of vertical boundaries targeting the zone of the dark ocean where most of the POC

161 fluxes attenuation occurs. At station PAP during cruise DY032, this so-called “Active  
162 Mesopelagic Zone” was located between 127 and 751 m.

### 163 **b) Carbon inputs**

164 The POC inputs to the active mesopelagic zone mainly involve the gravitational export of POC.  
165 Gravitational input was taken from Fuchs et al. (2022) who fitted a power law Martin curve (b  
166 of 0.84) on data obtained from 30 to 500m using Marine Snow Catcher (Belcher et al. 2016).  
167 However, gravitational input is not the only POC input known in the literature. Recently, Boyd  
168 et al. (2019), provided an estimation of other particle-injection pumps (PIPs) such as the mixed  
169 layer pump, physical pump, the seasonal lipid pump or the active transport related to metazoans  
170 migrations. At the PAP site during summer, only the eddy subduction pump, metazoans  
171 migrations, and large-scale physical pumps were relevant to take into account. Other PIPs do  
172 not correspond to the location and season considered in our study. From Boyd et al. (2019)  
173 review, these three particle-injection pumps seem to represent altogether around 52% of the  
174 gravitational export of POC. We therefore add up this proportion of POC to the purely  
175 gravitational inputs. This yields an overall POC flux of  $134 \text{ mg C m}^{-2} \text{ d}^{-1}$  exported into the  
176 active mesopelagic zone. The corresponding net POC input is  $117 \text{ mg C m}^{-2} \text{ d}^{-1}$  (that is POC  
177 fluxes at the end - 751 m - of the active mesopelagic zone subtracted to the one at the start -  
178 127 m - for PAP DY032).

179 DOC inputs are taken from Giering et al. (2014) and are considered as the sum of direct DOC  
180 export via physical processes (advection-diffusion) and active flux from zooplankton  
181 migrations. We estimated from their extended Data Fig. 2 that the DOC gradient below 100m  
182 is hardly visible meaning that physical vertical DOC export is insignificant for the active  
183 mesopelagic zone which is studied here. As a result, we set the DOC export at  $3 \text{ mg C m}^{-2} \text{ d}^{-1}$ ,  
184 which corresponds only to the active flux from zooplankton migrations from Giering et al.  
185 (2014).

### 186 **c) Carbon demands**

187 As explained above, prokaryotic carbon demand is generally assessed by adding rates of  
188 prokaryotic heterotrophic production (PHP) to that of prokaryotic respiration (PR). PHP of  
189 non-sinking prokaryotes (that is, free-living and attached to suspended particles prokaryotes)  
190 are derived from leucine incorporation measurements on seawater samples and are taken from  
191 Fuchs et al. (2022). These data did not permit the separation of the free-living from attached to  
192 suspended particles (Baumas et al. 2021). Hence, in the sequel, we no longer make this

193 distinction and group both types under the term “non-sinking prokaryotes”. During DY032,  
194 Marine Snow Catchers (MSC) were deployed to separate slow and fast-sinking particles from  
195 100L of samples (Riley et al. 2012; Baumas et al. 2021). PHP rates associated with prokaryotic  
196 communities of fast-sinking particles were taken from Baumas et al. (2021) and slow-sinking  
197 particles are presented here. Briefly, slow-sinking particle fractions were sampled in the 7L  
198 base of the MSC. Samples were incubated and leucine incorporation rates were measured as  
199 for fast-sinking particles in Baumas et al. (2021). The formula described in Baumas et al. (2021)  
200 was then applied to normalize to 100L as particles were concentrated in 7L after 2h of  
201 decantation and to remove the contribution of non-sinking prokaryotes which were **initially** in  
202 this compartment around slow-sinking particles of interest. Total sinking prokaryotes PHP  
203 rates were obtained by adding both fast-sinking and slow-sinking prokaryotes PHP rates. In  
204 addition, we were able to use the respiration rates of **fast-sinking particle-attached prokaryotes**  
205 particles **obtained at the PAP site during the DY032 cruise by** Belcher et al. (2016). For each  
206 depth (30-500m) the mean total O<sub>2</sub> consumption per particle in **nmol particle<sup>-1</sup>d<sup>-1</sup>** was converted  
207 to mg C m<sup>-3</sup> d<sup>-1</sup> (assuming a respiration quotient RQ(CO<sub>2</sub>/O<sub>2</sub>) = 1) by multiplying by the total  
208 number of particles (i.e. fecal pellets + phytoplanktonic aggregates) and dividing by 95L which  
209 is the volume of the MSC used (Riley et al. 2012). It is also important to note that PR for slow-  
210 sinking particles is missing. Thus, when we mention the respiration of sinking prokaryotes,  
211 only **fast-sinking particle-attached prokaryotes** are taken into account which certainly  
212 underestimates the respiration used. All prokaryotic carbon demand (PHPs and PRs) estimates  
213 were integrated within RUBALIZ boundaries (i.e. 127m - 751m). Non-sinking prokaryotes  
214 PHP rates were integrated using a piecewise model with a single node on the log-data as  
215 described in Fuchs et al. (2022). Sinking prokaryotes PHP rates were integrated using power  
216 law. Sinking PR were integrated using trapeze because data are only available until 500m and  
217 without any *a priori* on the curve shape, this method is certainly the most conservative.

218 Zooplankton activities are known to be related to POC concentration (Steinberg et al. 2008).  
219 Zooplankton respiration data were available only for the cruise D341 when the net POC input  
220 into the active mesopelagic layer was 59 mg C m<sup>-2</sup> d<sup>-1</sup> (including PIPs) instead of 134 mg C m<sup>-2</sup>  
221 d<sup>-1</sup> for DY032 (see above). For D341, zooplankton respiration integrated within the active  
222 mesopelagic zone (135-726m, Fuchs et al. 2022) was 9 mg C m<sup>-2</sup> d<sup>-1</sup>. Zooplankton respiration  
223 was integrated using a power law as in Giering et al. (2014). Zooplankton respiration data are  
224 missing for DY032, thus we consider this quantity as a percentage of the POC input that we  
225 calculate from the D341 data set, i.e. 14.67%. The zooplankton respiration value used here is  
226 therefore 17 mg C m<sup>-2</sup> d<sup>-1</sup>.

227 *Table 1: Fluxes and their associated values used in this study. Anderson & Tang model's terms*  
 228 *(Anderson and Tang 2010) corresponding to these fluxes are also shown. Values are integrated*  
 229 *between 127 and 751m which are boundaries of the active mesopelagic zone defined by Fuchs*  
 230 *et al. (2022). POC and DOC refer respectively to Particulate and Dissolved Organic Carbon,*  
 231 *PHP to Prokaryotic Heterotrophic Production, and PR to Prokaryotic Respiration.*

Name	Anderson and Tang's Model term correspondence	Values	units	sources
Net POC input	$Dlex$	117	mg C m <sup>-2</sup> d <sup>-1</sup>	Belcher et al. (2016); Boyd et al. (2019)
DOC input	$DOCex$	3	mg C m <sup>-2</sup> d <sup>-1</sup>	Giering et al. (2014)
Non-sinking prokaryotes PHP	$F_{BFL} + F_{BAD2}$	1.10E+07	pmol Leu m <sup>-2</sup> d <sup>-1</sup>	Baumas et al. (2021)
Sinking prokaryotes PHP	$F_{BAD1}$	1.02E+06	pmol Leu m <sup>-2</sup> d <sup>-1</sup>	Baumas et al. (2021)
Sinking prokaryotes PR	$R_{BAD1}$	19	mg C m <sup>-2</sup> d <sup>-1</sup>	Adapted from Belcher et al. (2016)
Zooplankton respiration	$R_{VA} + R_{VFL} + R_H + R_{Z1:6}$	17	mg C m <sup>-2</sup> d <sup>-1</sup>	Adapted from Giering et al. (2014)

232

## 233 **2.2 Mathematical methods**

### 234 **2.2.1 Parameter estimation**

235 The scope of our study is to estimate *in situ* parameters by inverting the model introduced by  
 236 Anderson and Tang (2010), adapted by Giering et al. (2014). We do not intend to present the  
 237 model in details here. The details of the equations constituting the version of the model used  
 238 can be found in the original paper (Anderson and Tang 2010), in the R code available at  
 239 <https://github.com/RobeeF/InverseCarbonBudgetEstim> and the specific terms related to  
 240 [variables used are reported in Table 1](#). The model is calibrated by choosing the set of input



241 parameters that yields the best fit between the model output and the data. As the model outputs  
242 85 outfluxes, we used a subset of four measurable outfluxes to calibrate the model: the PHP of  
243 non-sinking prokaryotes, the PHP of sinking prokaryotes, the PR of sinking prokaryotes and  
244 the respiration of zooplankton. These fluxes have been chosen because of their near direct  
245 correspondence with outputs of the model linked to the C demand of all groups (sinking  
246 prokaryotes, non-sinking prokaryotes, detritivores, bacterivores, and carnivores).

247 Similarly, the model relies on 20 input parameters (Table S1), which makes the parameter  
248 space of significant size and therefore challenging to explore. As such, we first determine the  
249 set of parameters that have the largest impact on the output of the model. Then for these  
250 parameters, the values that give the best fit between the data and the solution given by the  
251 model are determined.

#### 252 a) Sensitivity of the model to its inputs

253 In order to reduce the size of the input parameter space, Sobol Indices (Sobol 1993) were used  
254 to determine the most influential parameters. These indices enable quantification of the share  
255 of the variation of the output that can be imputed to each input parameter.

256 In essence, the first-order Sobol indices account for the direct influence of an input variable on  
257 the output. However, first-order Sobol indices neglect the interactions existing between this  
258 input variable and the other input variables. As such, in addition to the first-order Sobol Indices,  
259 we used the total Sobol indices introduced by Homma and Saltelli (1996) which encompass  
260 both the direct effect of a parameter and also its interactions with the other parameters.

261 First-order and total Sobol indices were computed to quantify the influence of each parameter  
262 over each of the four outfluxes. Only the parameters which had significant Sobol indices (i.e.  
263 Sobol indices  $> 0.20$ ) for at least one outflux were kept.

#### 264 b) Estimation of the parameters

265 The parameters which had no substantial effects on the output of the model were set to the  
266 values indicated by Anderson and Tang (2010) and Giering et al. (2014) and given in Appendix  
267 (Table S1). The other parameters were estimated by minimizing the distance existing between  
268 the four outfluxes predicted by the model and their *in situ* measured counterpart. The distance  
269 chosen here is a standardized Euclidean distance:

270

$$\sum_{i=1}^4 \left( \frac{\text{outflux}_{\text{obs},i} - \text{outflux}_{\text{model},i}}{\text{outflux}_{\text{obs},i}} \right)^2 \quad (1)$$

272 where  $\text{outflux}_{\text{obs},i}$  is the  $i$ -th measured flux and  $\text{outflux}_{\text{model},i}$  its modeled counterpart. The  
273 optimization method used is the Nelder-Mead algorithm (Nelder and Mead 1965): if the  
274 function to minimize depends on  $N$  variables (the number of input parameters here), a simplex  
275 constituted by  $N + 1$  points is defined. The coordinates of the simplex are updated in turn so  
276 that the simplex vertices get closer to the local minimum. Even if this method gives little  
277 theoretical guarantees of convergence, it has proven to work well in practice (Lagarias et al.  
278 1998) and has the advantage that it does not require computing the gradient of each outflux  
279 with respect to each input parameter.

280 As the model takes 20 inputs and outputs 85 fluxes, concerns might be raised about the  
281 uniqueness of the solution found to minimize the term (1). To make the model identifiable (i.e.  
282 sufficiently constrained to estimate the true value of the parameters), the number of input  
283 parameters to estimate is limited to the number of output fluxes available, here four. In this  
284 respect, the CFs have been fixed to  $0.5 \text{ kg C mol Leu}^{-1}$  (Estimates without fixing the CFs have  
285 however been carried out, see Table S4 in supp. data). This value, contrary to the previously  
286 classically used value of  $1.55 \text{ kg C mol Leu}^{-1}$  (Simon and Azam 1989; Nagata et al. 2010), was  
287 determined by Giering and Evans (2022) as the median value of 15 studies conducted in the  
288 mesopelagic zone. Doing so, we limit the number of free parameters to be estimated to four so  
289 that the model remains identifiable. The model is mostly linear and our experiments have  
290 shown the solution to be unique and independent of the initial values taken.

291 The codes and data to reproduce the results are available at  
292 <https://github.com/RobeeF/InverseCarbonBudgetEstim>

## 293 3.Results

### 294 3.1 Most sensitive parameters

295 Using Sobol indices, we identified the most sensitive parameters from the 20 of the Anderson  
296 and Tang (2010) model on the 4 fluxes outputs of the model for which we have the measured  
297 counterpart (i.e. PHP and PR of sinking prokaryotes, PHP of non-sinking prokaryotes and  
298 respiration of zooplankton). All parameter definitions are given in Table S1. For the outflux  
299 “PHP of non-sinking prokaryotes”, only the  $\text{PGE}_{\text{non-sinking}}$  appears to be sensitive with a Sobol

300 index of 0.68 meaning that it explains 68% of the variance (Table 2). Fluxes related to sinking  
301 prokaryotes, i.e. their PHP and their PR, appear to be highly influenced both by  $\Psi$ ,  $\alpha$ , and  
302  $PGE_{\text{sinking}}$ . For instance, our analysis yields to indices of 0.22 and 0.23 for  $\Psi$ , 0.24 and 0.24 for  
303  $\alpha$  and 0.27, 0.25 for  $PGE_{\text{sinking}}$  respectively. Surprisingly, zooplankton respiration is more  
304 impacted by the  $PGE_{\text{non-sinking}}$  (Sobol index of 0.52) than proper zooplankton parameters. All  
305 other parameters exhibit Sobol indices below 1%. Total Sobol indices, indicating the part of  
306 the variance of fluxes due to the parameter alone and in interaction with the others, were similar  
307 to the first-order indices, suggesting no interactions of parameters regarding the variance of  
308 fluxes. This sensitivity analysis enabled the identification of  $\Psi$ ,  $\alpha$ , and both PGEs as the most  
309 influential parameters, suggesting that their values should be set with particular care. Especially  
310 for the  $PGE_{\text{non-sinking}}$  which can be responsible for more than 50% of the variance of  $PHP_{\text{non-}}$   
311  $_{\text{sinking}}$  and zooplankton respiration. PGEs are growth efficiencies defined as the amount of new  
312 prokaryotic biomass produced per unit of organic C substrate assimilated and is a way to relate  
313 PHP and PR (del Giorgio and Cole 1998).  $\Psi$  corresponds to the percentage of POC consumed  
314 by prokaryotes and  $\alpha$  to the fraction of hydrolyzed POC which is lost into the surrounding  
315 water, i.e. not assimilated by sinking prokaryotes that hydrolyzed it.

316 *Table 2: First-order Sobol indices for the parameters of the model by Anderson and Tang*  
317 *(2010). The definition of each parameter can be found in Table S1. Significant Sobol indices*  
318 *(>0.2) are shown in red. PHP and PR respectively refer to Prokaryotic Heterotrophic*  
319 *Production and to Prokaryotic Respiration.*

	$\Psi$	$PGE_{\text{sinking}}$	$PGE_{\text{non-sinking}}$	$\alpha$	$\Phi_v$	$\beta_v$	$K_v$	$\Phi_v$	$\beta_v$	$K_v$	$\Phi_z$	$\beta_z$	$\lambda_z$	$K_z$	$\Phi_h$	$\beta_h$	$\lambda_h$	$K_h$	$\zeta$	$\zeta^2$
Non-sinking prokaryotes PHP	<0.01	0.021	0.681	0.01	<0.01	<0.01	<0.01	0.014	<0.01	0.011	-0.012	<0.01	<0.01	0.015	<0.01	<0.01	<0.01	<0.01	<0.01	<0.01
Sinking prokaryotes PHP	0.222	0.24	<0.01	0.265	<0.01	<0.01	<0.01	<0.01	0.011	<0.01	<0.01	<0.01	<0.01	<0.01	0.011	<0.01	<0.01	0.012	<0.01	-0.011
Sinking prokaryotes PR	0.225	0.243	<0.01	0.252	-0.019	<0.01	<0.01	<0.01	-0.011	<0.01	<0.01	<0.01	0.012	<0.01	<0.01	<0.01	<0.01	<0.01	<0.01	<0.01
Zooplankton respiration	<0.01	0.023	0.507	<0.01	<0.01	0.014	<0.01	0.064	0.027	0.041	<0.01	<0.01	<0.01	<0.01	<0.01	<0.01	0.028	<0.01	<0.01	<0.01

### 321 3.2 Model inversion

322

323 The optimization method, described in the material and method section, enabled the  
 324 determination of the 4 parameters identified as sensitive above:  $\Psi$ ,  $\alpha$ ,  $PGE_{\text{sinking}}$ , and  $PGE_{\text{non-}}$   
 325  $\text{sinking}$  in the case study of PAP DY032. Table 3 reports the combination found by model  
 326 inversion. By construction of the procedure (e.g. same number of input and output), the solution  
 327 is unique, explaining why no confidence intervals are reported. The errors between the four  
 328 fluxes generated by the model and their measured counterparts were less than 1%, far lower  
 329 than potential measurement errors. The zooplankton flux was the best matched, followed by  
 330 the PR of the sinking prokaryotes, the PHP of the non-sinking prokaryotes, and of the sinking  
 331 prokaryotes.

332

333 *Table 3: Estimation of the parameters  $\Psi$ ,  $\alpha$ ,  $PGE_{\text{sinking}}$  and  $PGE_{\text{non-sinking}}$  obtained by inversion*  
 334 *of the model by Anderson and Tang (2010). As the model was made identifiable, the solutions*  
 335 *are unique, explaining the absence of confidence intervals. The remaining differences between*  
 336 *the model outfluxes deriving from the estimated input values and the actual in situ*  
 337 *measurements are referred to as “Errors” and are expressed in percentage. PHP, PR, and ZR*  
 338 *respectively stand for Prokaryotic Heterotrophic Production, to Prokaryotic Respiration and*  
 339 *to Zooplankton Respiration.*

Estimations				Errors			
$\Psi$	$\alpha$	$PGE_{\text{sinking}}$	$PGE_{\text{non-sinking}}$	$PHP_{\text{non-sinking}}$	$PHP_{\text{sinking}}$	$PR_{\text{sinking}}$	ZR
0.675	0.777	0.026	0.087	-0.487%	0.524%	0.184%	-0.05%

340

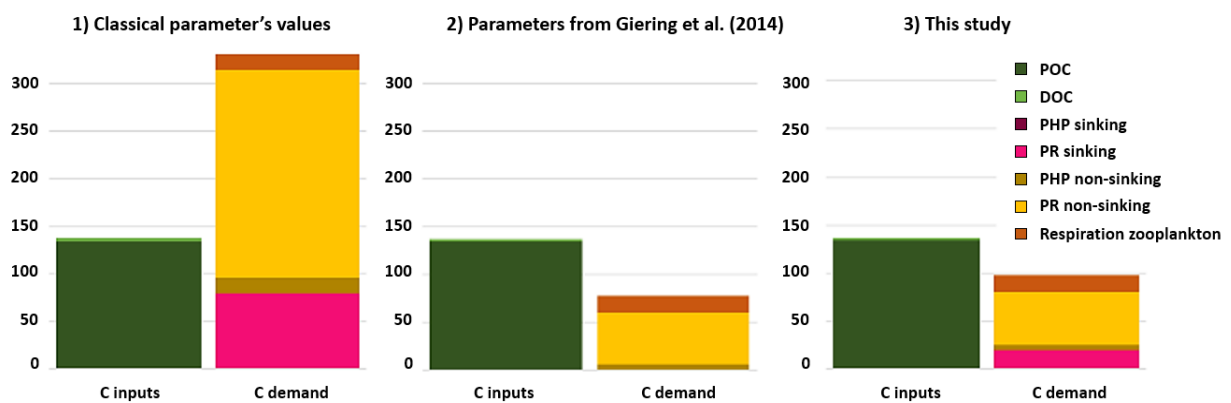
341

### 342 3.3 C budget

343

344 The two PGEs presented above along with CF of  $0.5 \text{ kg C mol Leu}^{-1}$  were applied to leucine-  
 345 incorporation rates measurements to build the corresponding active mesopelagic C budget. The  
 346 resulting C budget was compared with two other C budgets calculated with different sets of  
 347 parameters. The three active mesopelagic zone C budgets resulting from DY032 measurements  
 348 or estimation are represented in Fig. 1 with the budget (1) obtained with the classical CF value  
 349 of  $1.55 \text{ kg C mol Leu}^{-1}$  and median literature values for PGEs, i.e. 0.07 for  $PGE_{\text{non-sinking}}$   
 350 (Arístegui et al. 2005; Reinthaler et al. 2006; Baltar et al. 2010; Collins et al. 2015) and 0.02  
 351 for  $PGE_{\text{sinking}}$  (Collins et al. 2015); the budget (2) obtained with the parameter values from

352 Giering et al. (2014) who reconcile C budget, i.e. CF of 0.44 kg C mol Leu<sup>-1</sup>, PGE<sub>non-sinking</sub> of  
 353 0.07, and PGE<sub>sinking</sub> of 0.24 and the budget (3) obtained with a CF, PGE<sub>sinking</sub> and PGE<sub>non-sinking</sub>  
 354 of 0.5, 0.026 and 0.087, respectively, determined in this study. The combination yielding to the  
 355 largest discrepancy is the budget (1) (Fig. 1) (discrepancy of -194 mg C m<sup>-2</sup> d<sup>-1</sup>). The C input  
 356 seems to support the zooplankton respiration and total C demand of sinking prokaryotes but  
 357 not the one of non-sinking prokaryotes especially due to their PR of 218 mg C m<sup>-2</sup> d<sup>-1</sup>.  
 358 Combination of budget (2) and (3) presented both an excess of C (60 and 40 mg C m<sup>-2</sup> d<sup>-1</sup>  
 359 respectively) compared to the biological C demand. These two differ mainly on the PR of  
 360 sinking prokaryotes which is negligible in combination (2) but which is the second largest flux  
 361 in the C demand in our study. In all cases, the C demand of non-sinking prokaryotes accounts  
 362 for most of the total C demand.



363  
 364 *Figure 1: Carbon budget for the active mesopelagic zone estimation resulting from DY032*  
 365 *measurements or estimation and on which different combination of CF (1.55, 0.44 and 0.5 respectively*  
 366 *for budget 1) 2) and 3)), PGE<sub>sinking</sub> (0.02, 0.24 and 0.026 respectively for budget 1) 2) and 3)) and*  
 367 *PGE<sub>non-sinking</sub> (0.07, 0.08 and 0.087 respectively for budget 1) 2) and 3)) were applied on leucine*  
 368 *incorporation rates of sinking and non-sinking prokaryotes. See Fig. S1 for value details.*

## 369 4. Discussion:

370 As stated in the introduction, the scientific community has struggled to reconcile the  
 371 mesopelagic carbon budget with measurements and estimates showing a carbon demand often  
 372 greater than the amount of known organic C sources (e.g. Reinthaler et al. 2006; Steinberg et  
 373 al. 2008; Burd et al. 2010; Collins et al. 2015; Boyd et al. 2019). Building C budget involves a  
 374 plethora of parameters whose impacts are overlooked and often neglected, mainly because  
 375 neither their ideal values nor their underlying mechanism in the water column across space and  
 376 time are clearly understood. The scientific community is concerned about this issue (e.g. Burd  
 377 et al. 2010; Giering and Evans 2022), but in the absence of a better option and in an attempt to

378 encourage comparisons, the same parameter values are universally used. A first step towards  
379 this direction was conducted thanks to the RUBALIZ method (Fuchs et al. 2022) which  
380 precisely determines the vertical location of the “active mesopelagic zone” and thereby  
381 estimates the boundaries between which to integrate C fluxes. In the current study, we pursue  
382 this investigation and combine measurements with modeling approaches to investigate the role  
383 of sensitive parameters related to the remineralization of POC in the mesopelagic zone.

#### 384 **4.1 Optimization method: Consistency of parameters estimated**

385 The Anderson and Tang (2010) model takes as inputs the measured C inputs as well as 20  
386 parameters related to the activity of organisms such as sinking prokaryotes, non-sinking  
387 prokaryotes, zooplankton detritivores, bacterivores, and carnivores. Among the 20 parameters,  
388 four have been found to be particularly sensitive in assessing the carbon demands of the various  
389 groups:  $\Psi$  (percentage of particle consumption by prokaryotes),  $\alpha$  (percentage of C hydrolyzed  
390 released in surrounding water),  $PGE_{\text{non-sinking}}$  and  $PGE_{\text{sinking}}$  (growth efficiencies of sinking and  
391 non-sinking prokaryotes). It is interesting to note that zooplankton respiration (which is the  
392 sum of detritivores, bacterivores and carnivores respiration) is mostly sensitive to one  
393 parameter:  $PGE_{\text{non-sinking}}$  but not to a parameter specific to zooplankton. This counter-intuitive  
394 result suggests a strong synergy between the two model compartments. At this point, it is  
395 challenging to establish whether this is the outcome of a complex ecological process or a model  
396 artifact.

397  
398 In the model, the consumption of particles is done by two groups: prokaryotes ( $\Psi$ ) and  
399 detritivores ( $1-\Psi$ ). It can be estimated by taking the average ratio between PHP and ZR.  
400 Anderson and Ryabchenko (2009) estimated  $\Psi$  using calculations of POC consumption by  
401 prokaryotes and zooplanktons between 150 and 1000m performed by Steinberg et al. (2008) in  
402 the Pacific. Following this, they set  $\Psi$  at 0.76. The inversion of the Anderson and Tang model  
403 (2010) leads to a well-identified solution of  $\Psi$ , i.e. 0.67 in the case of PAP DY032 cruise. This  
404 value is in line with the one used by Anderson and Tang (2010). However, data are lacking to  
405 compare and explore variations of  $\Psi$  value across seasons, locations or depths. In the model,  $\Psi$   
406 participates in the repartition of POC input between prokaryotes and detritivores. Whether for  
407 modeling purposes to determine  $\Psi$  or to build a C-budget without a model, PHP and ZR are  
408 required. It remains too rare to have both together and more future efforts should be devoted to  
409 get PHP and ZR concomitantly.

410

411 Beyond  $\Psi$ , according to Sobol indices,  $\alpha$  is the second parameter of interest. ~~Amino acids and~~  
412 ~~sugar are major components of POC, constituting between 40 to 70% of POC in the~~  
413 ~~mesopelagic zone (Wakeham et al. 1997).~~ When prokaryotes consume POC using hydrolytic  
414 enzymes, a major fraction of the hydrolyzed C is lost to the surrounding environment as DOC  
415 (Smith et al. 1992; Vetter et al. 1998). This loss is represented by  $\alpha$  and is very difficult to  
416 quantify accurately. Two major experiments, focused on amino acid hydrolysis, aimed to  
417 determine such losses: Smith et al. (1992) and Grossart and Ploug (2001). Smith et al. (1992)  
418 sampled particles at 25m and showed that 97% of particulate combined amino acids are  
419 released in the surrounding water. Later, Grossart and Ploug (2001) using aggregates from  
420 phytoplankton cultures show a loss of POC of 74%. Relying on these two studies, Anderson  
421 and Tang (2010) followed by Giering et al. (2014) consider that the value should be lower than  
422 that of a fresh detritus and choose a conservative value of 0.5. In the case of these two  
423 experiments, only the amino acids are considered and the experiments were conducted under  
424 laboratory-controlled settings. ~~However, both, amino acids and sugar are major components of~~  
425 ~~POC, constituting between 40 to 70% of POC in the mesopelagic zone (Wakeham et al. 1997).~~  
426 Conversely, we used unpublished data from PEACETIME cruise (see methods details in supp.  
427 data) of *in situ* hydrolysis rates of aminopeptidase and  $\beta$ -glucosydase from sinking prokaryotes  
428 (which hydrolyze amino acids and sugar, respectively) that we were able to convert into  
429 hydrolyzed carbon fluxes (see measurements and calculation details in supp. data).  
430 Unfortunately, total hydrolyzed C fluxes were most of the time below the C demand of the  
431 sinking prokaryotes which is unrealistic and probably due to the low amount of POC (sinking  
432 POC concentration of  $<1 \text{ mg L}^{-1}$  in the sinking fraction) resulting in insufficient sinking  
433 prokaryotes abundance to detect their activity by volume. However, when total hydrolyzed C  
434 fluxes were superior to  $\text{PHP}_{\text{sinking}}$  (indicating that some hydrolyzed C is not assimilated and is  
435 released),  $\alpha$  was estimated between 0.19 and 0.79 with a mean of  $0.41 \pm 0.24$  and seems to  
436 decrease with depth (see calculations details in supp data). This could confirm Grossart and  
437 Ploug's (2001) work showing that the older a detritus is, the less enzymatic activity there is  
438 and therefore the less amino acid loss. Even if  $\alpha$  is not measurable easily, this parameter is  
439 identified at 0.78 by the inversion method during a post-bloom period at the PAP site. This  
440 value is consistent with Smith et al. (1992) and Grossart and Ploug (2001) evidencing high  $\alpha$   
441 for surface aggregates (0.97) with laboratory-made phytoplankton aggregates (0.74), or with  
442 our calculations for the Mediterranean Sea ( $0.41 \pm 0.24$ ), an oligotrophic region. This suggests  
443 that the optimization method is a relevant alternative to determine  $\alpha$ . In addition,  $\alpha$  corresponds  
444 to a release of C in the surrounding water. Regarding the model, the C demand of free-living

445 prokaryotes matches the hydrolyzed C released which constitutes their main C sources. The  
446 relationship between enzymatic activities and heterotrophic production of free-living  
447 prokaryotes is well documented in the deep-sea ocean (Cho and Azam 1988; Smith et al. 1992;  
448 Hoppe and Ullrich 1999; Tamburini et al. 2002, 2003; Nagata et al. 2010). Total C demand of  
449 non-sinking prokaryotes is challenging to measure due to the diversity of existing methods,  
450 especially the PR (e.g. Table S2), which leads to an incredibly wide range of estimated values.  
451 Subsequently, identifying  $\alpha$  via the optimization method could help to avoid these conflicting  
452 PR measurements.

453

454 The last two sensitive parameters according to Sobol indices were  $PGE_{\text{non-sinking}}$  and  $PGE_{\text{sinking}}$ .  
455 A wide range of  $PGE_{\text{non-sinking}}$  has been estimated using  $PHP_{\text{non-sinking}}$  and  $PR_{\text{non-sinking}}$  in the open  
456 ocean (e.g. Sherry et al. 1999; Lemée et al. 2002; Carlson et al. 2004; Arístegui et al. 2005;  
457 Reinthaler et al. 2006; Baltar et al. 2009, 2010; Collins et al. 2015). Overall it varies from 0.001  
458 to 0.64 (Collins et al. (2015) and Sherry et al. (1999), respectively). However, these values  
459 were produced from different protocols for the PHP (changes in biomass, thymidine or leucine  
460 incorporation, each with its own conversion factors and/or constants) and for the PR methods  
461 (by ETS measurements, micro-winkler titration, changes in dissolved  $O_2$ , or using optodes  
462 sensors spots, see Table S2) and correspond to various locations, seasons and depths. These are  
463 all valid reasons that can potentially explain the stark contrast in the values reported. If one  
464 focuses only on the mesopelagic zone in the North Atlantic, the median is 0.07 (Arístegui et al.  
465 2005; Reinthaler et al. 2006; Baltar et al. 2010; Collins et al. 2015). The optimization method  
466 yielded to a value of 0.087 and therefore produces very consistent results for a post-bloom  
467 period at the PAP site. Concerning  $PGE_{\text{sinking}}$ , too few values are available. To our knowledge,  
468 only Collins et al. (2015) provided *in situ* values associated with sinking prokaryotes (from  
469 0.01 to 0.03) at 150m. This is the only comparison we have, and our value of 0.026 matches  
470 this order of magnitude. As a further comparison, the non-integrated data from DY0312 allows  
471 us to calculate a  $PGE_{\text{sinking}}$  (using  $PGE_{\text{sinking}} = PHP_{\text{sinking}} / (PHP_{\text{sinking}} + PR_{\text{sinking}})$ ) according to del  
472 Giorgio and Cole (1998). The result is thus, a depth-specific PGE instead of a depth-integrated  
473 PGE. This led to a variation from 0.033 at 70m to 0.0013 at 500m. Although the lack of  
474 datapoints deeper than 500m and the low number of points forces us to stay cautious about  
475 these estimates, it may indicate that  $PGE_{\text{sinking}}$  is not constant throughout the mesopelagic zone  
476 and decreases with depth. Constraining conditions due to the increase of hydrostatic pressure  
477 and decrease in temperature experienced by prokaryotes attached to sinking particles could  
478 explain this decrease in  $PGE_{\text{sinking}}$  (Stief et al. 2021; Tamburini et al. 2021). Under highly  
479 constrained conditions, Russell and Cook (1995) explained that maintaining respiration at the



480 highest possible rate would allow the supply of active membrane transporters which are vital  
481 to the cell. This implies a low but optimal PGE (Westerhoff et al. 1983) which could thus  
482 decrease with depth and time as the POC becomes less labile (Grossart and Ploug 2000). On  
483 the contrary, the Anderson and Tang (2010) model, and the associated model inversion  
484 presented here, is built so that the mesopelagic zone is considered as one homogeneous entity.  
485 Explicitly, specifying depth-dependent  $PGE_{\text{sinking}}$  in the mesopelagic zone could lead to more  
486 realistic modeling, but would entail a non-negligible additional model complexity.

487

488 It is worth noting that the  $PGE_{\text{sinking}}$  and  $PGE_{\text{non-sinking}}$  estimated here rely on a leucine-to-carbon  
489 Conversion Factor (CF) of  $0.5 \text{ kg C mol Leu}^{-1}$ . This value comes from the median of 15 values  
490 obtained on the free-living prokaryotes of the mesopelagic zone (between 300 to 1000m),  
491 which do not sink and are adapted to their place in the water column (Giering and Evans 2022).  
492 However, to our knowledge, there are no such values measured for the specific case of sinking  
493 prokaryotes. The latter are surface prokaryotes that have attached to the particles and will  
494 experience changes in conditions (e.g. pressure, temperature) linked to their sink (Baumas et  
495 al. 2021; Tamburini et al. 2021). The CF depends, among other things, on the leucine fraction  
496 in the proteins and the cellular carbon/protein ratio (Kirchman and Ducklow 1993). It is known  
497 that stresses can affect the incorporation of leucine into proteins and general protein production  
498 (e.g. Young 1968; Welch et al. 1993) and that these parameters can vary with prokaryotic  
499 diversity, especially between bacteria and archaea (Bogatyeva et al. 2006). Stresses occur  
500 during the descent throughout the water column and sinking prokaryotes experienced a drastic  
501 decrease in diversity following the sink at PAP DY032 (Baumas et al. 2021; Tamburini et al.  
502 2021). We can therefore easily imagine that the CF for sinking prokaryotes could be impacted.  
503 Despite this, without having further data, we applied the same CF on sinking as the 0.5  
504 recommended by Giering and Evans (2022) for non-sinking prokaryotes **and the results were**  
505 **consistent.**

506

## 507 **4.2 Influence on mesopelagic C Budget**

508 As stated in the introduction, mesopelagic C budgets are constructed by applying a CF and a  
509 PGE on leucine incorporation rates data to assess prokaryotic C demand. In Fig. 1, we applied  
510 three different combinations of CFs and PGEs to the same data. The combination using  
511 conventional CF of  $1.55 \text{ kg C mol Leu}^{-1}$ ,  $PGE_{\text{non-sinking}}$  of 0.07, and  $PGE_{\text{sinking}}$  of 0.02 led to an aberrant  
512 discrepancy such that more than the entire C pool would be remineralized in the active  
513 mesopelagic zone and that there would be no source of C to sustain deeper zone life nor

514 sequestration by the BCP. As stated above, this was a recurrent issue in the field (Reinthal et  
515 al. 2006; Steinberg et al. 2008; Burd et al. 2010; Collins et al. 2015; Boyd et al. 2019) with the  
516 exception of Giering et al. (2014) who reconcile the C budget of the mesopelagic zone. Giering  
517 et al. (2014) results were mainly due to the difference in CF applied on their data, i.e. 0.44 kg  
518 C mol Leu<sup>-1</sup>. However, from a model point of view, the main difference between C budgets  
519 estimated using Giering et al. (2014) parameters and those determined by our optimization  
520 method is due to the 10-fold difference between PGE<sub>sinking</sub> used. Giering et al. (2014) used 0.24  
521 which is the mean of a 14 days incubation experiment during which PGE varied from 0.45 in  
522 the first 3 days to 0.04 at the end for riverine aggregates (Grossart and Ploug 2000). Despite  
523 the fact that PGE<sub>sinking</sub> data are very scarce, riverine values of 0.24 seem highly unlikely and  
524 inappropriate to mesopelagic sinking prokaryotes compared to what is known in marine  
525 environments (e.g. Collins et al. 2015). Indeed, if we consider that enzymes account for a large  
526 proportion of the proteins produced by cells (see above) the PGE<sub>sinking</sub> must be low due to the  
527 high metabolic cost of their production (Grossart and Ploug 2000). Finally, the C budget built  
528 from a combination of CFs of 0.5 kg C mol Leu<sup>-1</sup> and PGEs revealed by our optimization method  
529 seems the most reasonable option (from the three budgets built, Fig. 1) with an excess of C  
530 input of 40 mg C m<sup>-2</sup> d<sup>-1</sup>. In this case, PGEs were determined by the model, which in addition  
531 to PHP and PR of sinking and non-sinking prokaryotes and zooplankton respiration, also  
532 accounts for the production of zooplankton biomass into calculations. We do not have  
533 measurements or estimates for the production of zooplankton biomass but based on the model,  
534 this biomass production is 11 mg C m<sup>-2</sup> d<sup>-1</sup>. Adding this value to the C demand implies a leftover  
535 of 29 mg C m<sup>-2</sup> d<sup>-1</sup> that is not used and is exported below the active mesopelagic zone via  
536 gravitational sinking POC. This value is in accordance with the POC flux estimated from  
537 measures at 751m (thus at the exit of our zone): 17 mg C m<sup>-2</sup> d<sup>-1</sup>. Being aware of the biases that  
538 may exist in the fluxes used as well as in the construction of the model itself, our optimization  
539 method enables the determination of realistic values of parameters and thus constructing robust  
540 C budgets. As far as we know, the combination of field measurements (using consistently  
541 defined integration depths, such as RUBALIZ (Fuchs et al. 2022) with the use of optimization  
542 method on the Anderson & Tang model has led to the most complete and realistic mesopelagic  
543 carbon budget.

544

### 545 **4.3 Model: reliability and potential biases**

546 The Anderson and Tang model (Anderson and Tang 2010) was originally parametrized with  
547 20 input parameters and 85 output fluxes, and is hence by definition an underdetermined model

548 as the number of outputs is higher than the number of inputs. To make the model identifiable,  
549 i.e. obtaining unique solutions for each parameter value, the number of parameters allowed to  
550 vary, namely:  $\Psi$ ,  $\alpha$ ,  $PGE_{\text{non-sinking}}$ , and  $PGE_{\text{sinking}}$ , was restricted to the number of measurable  
551 outputs (here four,  $PHP_{\text{sinking}}$ ,  $PR_{\text{sinking}}$ ,  $PHP_{\text{non-sinking}}$ , and zooplankton respiration).  
552 Measurement errors (e.g. measurement device errors, *in situ* variabilities, errors due to  
553 integration methods) are typically challenging to characterize. Furthermore, even if these four  
554 outfluxes well describe the prokaryotic and zooplankton compartment fluxes, one may wonder  
555 about the sensitivity of the results to the fact that a given outflux is not available or estimated  
556 with error.

557

558 As a result, we have tested two settings: a model inversion without the zooplankton respiration  
559 flux (using only three fluxes) and a second setting where the PGEs were estimated from the  
560 leucine incorporation rate using freely varying CFs, i.e. with CFs no more fixed at 0.5 as a  
561 value. The results are reported in Table S3 and S4. Not using the zooplankton flux to inverse  
562 the model mechanically adds some variability to the estimation results, especially concerning  
563  $\Psi$ ,  $\alpha$ , and  $PGE_{\text{non-sinking}}$ , in decreasing order of variability (Table S3). The  $PGE_{\text{sinking}}$  was not  
564 affected as its confidence interval length was inferior to  $10^{-7}$ : this underlines the very limited  
565 influence between the zooplankton and sinking prokaryote compartments in the model  
566 (contrary to the zooplankton and non-sinking prokaryote compartments). Yet, the difference  
567 between the four-flux and three-flux parameter estimations was negligible (<1% variation for  
568 each estimate), highlighting the robustness of the estimates to the potential unavailability of  
569 the zooplankton respiration. On the contrary, as made visible in Table S4, not fixing the CFs  
570 to estimate the PGEs created more variations in the PGE estimations, while the estimations of  
571  $\Psi$  and  $\alpha$  changed by less than 5% with respect to Table 2 estimations. The PGEs of the attached  
572 and free-living parameters get significantly closer to their fixed boundaries (10%), while the  
573 CFs rise, especially the CF of the attached particles ( $=1.87 \text{ kg C mol Leu}^{-1}$ ). Similarly, if PGEs  
574 are no longer bounded, the estimates of PGEs (0.17 for attached prokaryotes and 0.23 for free-  
575 living prokaryotes) and CFs ( $3.93 \text{ kg C mol Leu}^{-1}$  for attached prokaryotes and  $1.53 \text{ kg C mol}$   
576  $\text{Leu}^{-1}$  for free-living prokaryotes) become unrealistic. This can be explained by the fact that the  
577 PGEs and CFs play similar **mathematical roles** in the current formulation of the model. Hence,  
578 without additional fluxes ensuring full model identifiability, one of these two types of  
579 quantities needs to be fixed to estimate the other.

580

581 In addition to these sensitivity analyses, an uncertainty analysis has been run by simulating  
582 errors in the measurements of the POC, DOC and the four output fluxes (see Table S5 in supp.

583 data). Simulating errors from -10% to 10% for each flux, the estimation of the four parameters  
584 of interest were lowly affected: 1%, 2%, 3% and 1% on average for the  $\Psi$ ,  $PGE_{\text{sinking}}$ ,  $PGE_{\text{non-}}$   
585  $\text{sinking}$  and  $\alpha$ , respectively. The  $PGE_{\text{non-sinking}}$  was mostly sensitive to measurement errors of POC  
586 flux, DOC flux and  $PHP_{\text{non-sinking}}$  (generating variations of 6%, 5% and 5%, respectively).  
587 Similarly, the  $PGE_{\text{sinking}}$  was logically mostly sensitive to errors in the  $PHP_{\text{sinking}}$  and  $PR_{\text{sinking}}$   
588 (generating variations of 6% for both). For the measurement errors, the generated variations all  
589 remained under 3% which is reassuring concerning the stability of the estimation.

590

591 Finally, the last potential source of estimation bias results from the assumed stationarity  
592 hypothesis of the mesopelagic system. For logistical and technical reasons, measurements and  
593 sampling between the upper and lower boundary of the mesopelagic zone are typically  
594 performed simultaneously. The stationarity assumption is thus a natural foundation ground  
595 upon interpretations and models. However, there is a temporal delay in flux variations between  
596 the upper layer and lower measurements (Giering et al. 2017; Stange et al. 2017). This delay  
597 depends on the particles sinking speed typically ranging from 2 to 1500 m d<sup>-1</sup> (Alldredge and  
598 Silver 1988; Armstrong et al. 2002; Trull et al. 2008; Turner 2015), their morphotype, density  
599 and porosity as well as the timing of their production. Strong meteorological events can also  
600 perturbate C fluxes from the water column with an increasing time lag over depth (e.g. Pedrosa-  
601 Pàmies et al. 2019). Admittedly, C budgets suffer from lack of time integration into the  
602 analysis. Our study regarding PAP site is also concerned as it undergoes a substantial  
603 seasonality (Cole et al. 2012; Giering et al. 2017). Although, we do not have enough  
604 understanding of vertical time lag to change the model and to avoid such bias yet. Some long-  
605 term observatories such as BATS in the Bermuda Atlantic or HOT in Hawaii provide  
606 biogeochemical flux time series but monthly sampling focuses mostly on the euphotic zone  
607 and does not investigate the mesopelagic zone enough. Sampling at discrete times following  
608 the sink of a bloom (e.g. Le Moigne et al. 2016) could be a solution, which would nevertheless  
609 entail a significant cruise planning effort.

610

#### 611 **4.4 Grounds for improvements**

612 Anderson & Tang model allowed us to have a comprehensive vision of the remineralization  
613 processes in the mesopelagic zone by including the interactions between various  
614 compartments, completing *in situ* measurements with a comprehensive vision of the  
615 mechanisms at stake. The described inversion of the Anderson & Tang model provided  
616 meaningful estimations of the parameters of interest. However, as most models represent

617 complex phenomena, some processes are not fully and properly captured by the model. Below,  
618 we provide a list of processes that may help refining mesopelagic C budget estimations.

619

#### 620 **4.4.1 Other microorganisms**

621 **The role of microbial eukaryotes, viruses, and the input of C by chemolithotrophs (Herndl and**  
622 **Reinthalder 2013; Lara et al. 2017; Kuhlisch et al. 2021; Luo et al. 2022) are not included in the**  
623 **model.** For instance, eukaryotes can dominate microbial biomass on bathypelagic particles  
624 (Bochdansky et al. 2017), and have the potential to promote the aggregation of particles (Jain  
625 et al. 2005; Chang et al. 2014; Hamamoto and Honda 2019; Xie et al. 2022). Viruses could be  
626 the main cause of prokaryotic and phytoplanktonic mortality. Thus, DOC fluxes could be  
627 attributed to them, in particular with the cell lyses they provoke (Fuhrman 2000 and ref within,  
628 Lara et al. 2017; Kuhlisch et al. 2021). In the North Atlantic, 9 to 12% of cells could be infected  
629 by viruses which would cause a DOC production of  $0.1 \text{ mg C m}^{-3} \text{ d}^{-1}$  (Wilhem and Suttle 1999).  
630 For comparison, PHP results on PAP before integration (with a conversion factor of  $0.5 \text{ kg C}$   
631  $\text{mol}^{-1} \text{ Leu}$ ) were mostly below this value. In addition, inorganic C fixation by chemoautotrophy  
632 would be of the same order of magnitude as  $\text{PHP}_{\text{non-sinking}}$  rates (Herndl et al. 2005; Reinthalder  
633 et al. 2010). It would be important to verify what microbial eukaryotes, chemolithotrophs or  
634 viruses contributions are, even if the poor understanding of these processes currently prevents  
635 properly integrating them into models.

636

#### 637 **4.4.2 Lifestyles**

638 More surprisingly, sinking prokaryotes are poorly considered as they are not sampled with the  
639 Niskin bottles classically used in oceanography (Planquette and Sherrell 2012; Baumas et al.  
640 2021). However, the use of the MSC at PAP DY032 allows us to access fractions of particulate  
641 organic carbon that will allow us to evaluate the importance of sinking prokaryotes. We have  
642 seen that their C demand is not negligible and represents 18% of total C demand. Anderson &  
643 Tang model distinguishes sinking particles from neutrally buoyant particles, each with distinct  
644 attached communities. Since sampling with MSC only allows us to separate what is sinking  
645 from what is not, we merged free-living prokaryotes with those attached to neutrally buoyant  
646 particles without distinction. However, unlike free-living prokaryotes, prokaryotes attached to  
647 neutrally buoyant particles have access to POC and must produce enzyme activity with  
648 different metabolisms than their free-living counterparts. On the other hand, prokaryotes  
649 attached to neutrally buoyant particles are also different from prokaryotes attached to sinking  
650 particles since they do not undergo changes in temperature and pressure related to the sink.

651 They must therefore surely have intrinsically different PGE and associated remineralization  
652 rates. It would therefore be valuable to consider them as a third distinct group in laboratory  
653 experiments and sampling. Contrary to the sinking or ascending particles which are naturally  
654 split by their sinking/ascending velocity (e.g. respectively Smith et al. 1989; Cowen et al. 2001;  
655 McDonnell et al. 2015), no means allow the selective and exclusive sampling of neutrally  
656 buoyant particles. The only valid way is to use the MSC to let the sinking particles fall into the  
657 lower compartments and to filter the "non-sinking" part to retain the particulate fraction.  
658 However, it is known that filtration affects the activities of prokaryotes and generates biases  
659 (Edgcomb et al. 2016). This makes investigations of prokaryotes associated with neutrally  
660 buoyant particles particularly challenging and future endeavors should urgently attempt to  
661 target them.

662

#### 663 **4.4.3 OC inputs**

664 Continuing in the same line, the inputs of C that the model takes into account are only the  
665 gravitational POC and the DOC. We chose to artificially increase the gravitational POC flux  
666 to add sources of neutrally buoyant particles in the form of PIPs (eddy subduction pump,  
667 metazoans migrations and large-scale physical pumps). Indeed, Boyd et al. (2019) clearly  
668 showed that these PIPs can be of paramount importance (here we have estimated them at 51.6%  
669 of the gravitational flux). ~~Accounting for these neutrally buoyant particles through the POC  
670 flux was performed due to the model structure.~~ Yet, explicitly describing them in a dedicated  
671 compartment of the model could be an improvement for future research, as these neutrally  
672 buoyant particles have an effect on the whole system, including the prokaryotes linked to  
673 various types of particles and their predators or on particle fragmentation. Given the existence  
674 of the neutrally buoyant particle compartment, it is feasible to adapt the model to account for  
675 these C inputs. This is even more relevant as new optical instruments have flourished (e.g.  
676 Briggs et al. 2013; Giering et al. 2020; Picheral et al. 2022) and would make it easier to better  
677 quantify these neutrally buoyant particle fluxes.

678

679

680

681

682

683

684

#### 685 4.4.4 *In situ* pressure effect

686 Our last major concern deals with the fact that neither Niskin nor MSC avoid disruption  
687 introduced through the process of depressurization when samples are collected at depth  
688 (Tamburini et al. 2013; Garel et al. 2019). Heterotrophic activities associated to non-sinking  
689 prokaryotes are known to decrease with depth but were mostly sampled without taking care of  
690 the *in situ* pressure (e.g. Turley and Mackie 1994; Arístegui et al. 2009). From our knowledge,  
691 some devices such as the IODA<sub>6000</sub> (Robert 2012) were specifically designed to measure *in situ*  
692 PR of non-sinking prokaryotes. However, enigmatically high PR values (2-3 orders of  
693 magnitude higher than PHP) are measured by IODA<sub>6000</sub>, making it difficult to have confidence  
694 in these *in situ* measured PR rates. During the PEACETIME cruise, we use a pressure-retaining  
695 sampler (methods presented in supp data), allowing for the first time to access both PHP<sub>non-</sub>  
696 <sub>sinking</sub> and PR<sub>non-sinking</sub> rates and to compare it with classical depressurization procedures (Fig.  
697 S1). We observed that activity rates of non-sinking prokaryotes kept under pressure were  
698 always higher when kept at *in situ* hydrostatic pressure than their decompressed counterparts  
699 and, surprisingly, seem to increase with depth rather than decrease typically depicted and found  
700 when the samples are decompressed (Fig. S1). ~~Focusing on PR<sub>non-sinking</sub> rates, obtained values~~  
701 ~~are also several orders of magnitude too high to be realistic in regard to C Budgets and prevent~~  
702 ~~us from calculating PGEs. As PHP and PR are linked, it is very likely that the pressure effect~~  
703 ~~(here, an increase) is reflected on both and thus in the associated PGE<sub>non-sinking</sub>. Taking~~  
704 ~~hydrostatic pressure into account could thus drastically affect C budgets and even for~~  
705 ~~zooplankton respiration as we saw in the model that they are really sensitive to PGE<sub>non-sinking</sub>.~~  
706 ~~We highly recommend using either direct *in situ* measurements or pressure retaining systems~~  
707 ~~for future research. This advice should be followed carefully, especially from 500m where the~~  
708 ~~pressure effect starts to be very important (Fig. S1), while the piezosphere was previously~~  
709 ~~considered below 1000m depth (Jannasch and Taylor 1984; Yayanos 1986). Furthermore, this~~  
710 ~~shows the crucial interest to measure points below 500m in order to get a global trend of the~~  
711 ~~profile, which could not have been done here for sinking prokaryotes (the MSC were deployed~~  
712 ~~only up to 500m during the cruise DY032).~~ From a C-budget point of view, taking *in situ*  
713 pressure into account will increase C demand of free-living prokaryotes well adapted to their  
714 living depth.

715

716 The effect of pressure acts inversely on sinking prokaryotes, as they are surface prokaryotes  
717 (unadapted to high-hydrostatic pressure) that undergo a dynamic pressure increase as the  
718 particle sinks (Baumas et al. 2021; Tamburini et al. 2021). Besides, repeated results (Tamburini  
719 et al. 2006, 2009, 2021; Riou et al. 2018) have shown that, while performing a sinking

720 simulation experiment the activities of sinking prokaryotes are affected during the sink. For  
721 instance, they noticed that the aminopeptidase activity was always lower with increasing  
722 pressure over time than at atmospheric pressure on diatom aggregates (Tamburini et al. 2006).  
723 This may reflect the stress endured by the sinking prokaryotes as they experience the sink. This  
724 could also be another explanation of why the fraction of hydrolyzed C released ( $\alpha$ ) tends to  
725 decrease with depth as it is directly linked with aminopeptidase activity. In view of these  
726 statements, it is not surprising that the PHP and PR, and therefore a PGE, are impacted by  
727 increasing pressure (e.g. Stief et al. 2021; Tamburini et al. 2021). Only the RESPIRE from  
728 Boyd et al. (2015) provides *in situ* measurements of the PR of sinking prokaryotes. However,  
729 in line with the previous comments, it gives unrealistically rather high values. Thus, sinking  
730 simulation experiments remains, in the present, the best alternative to understand the mechanics  
731 of sinking prokaryotes during the sink of their associated particle. Several systems exist to  
732 simulate the sink (e.g. de Jesus Mendes et al. 2007; Grossart and Gust 2009; Tamburini et al.  
733 2009; Mendes and Thomsen 2012; Dong et al. 2018; Stief et al. 2021; Liu et al. 2022), all  
734 showing a general tendency that hydrostatic pressure affects activities (and diversity) of  
735 surface-originated prokaryotes, decreasing the integrated C demand when taking into account.  
736 Handling high-pressure sampling or experiments requires much more effort and material than  
737 usual methods. However, it seems highly worthy when investigating both, sinking and non-  
738 sinking prokaryotes activities, in regard to C-budget purposes.

739

## 740 5. Conclusion

741 By combining *in situ* data from the DY032 cruise at the PAP site with inversion of the  
742 Anderson & Tang model which includes known processes from the biological C pump, we  
743 provide robust and ecologically realistic estimates of key parameters and to better characterize  
744 the patterns at stake.

- 745 1) We showed that the most sensitive parameters in the model are the ones related to  
746 prokaryotes such as prokaryotic growth efficiencies, leucine to carbon conversion  
747 factor, and C hydrolyzed by sinking prokaryotes released to the surrounding water.
- 748 2) By inversion of Anderson and Tang's model, we determined consistent values of the  
749 parameters listed above.





771 *prokaryotes. In turn, viruses and chemoautotrophs can increase the amount of usable labile C.*  
772 *Quantifying C demand and role on POC fluxes of these different groups is crucial to truly assess C*  
773 *sequestration in the deeper layer of the water column. However, a multitude of uncertainties remains*  
774 *for each group. The quantities enclosed in green are well known, in blue lack data and in pink are*  
775 *unknown. C demand is the sum of heterotrophic production (PHP) and respiration (PR). The*  
776 *understanding of these two quantities is currently better for the free-living prokaryotes whereas data*  
777 *are still insufficient for sinking prokaryotes and even absent for prokaryotes attached to non-sinking*  
778 *particles. Moreover, to build C budgets, these variables are integrated over a few hundred meters of*  
779 *water column and the relationship between in situ pressure and C demand remains often neglected even*  
780 *if this relationship highly depends on the prokaryote type considered (not constant for sinking*  
781 *prokaryotes unadapted to the increased pressure, constant for free-living prokaryotes well adapted to*  
782 *their living depth and constant for prokaryotes attached to non-sinking particles which can be adapted*  
783 *or not if the particle was sinking before being stopped in its sink ).*  
784

## 785 **Code/Data availability**

786 The codes and data to reproduce the results are available at  
787 <https://github.com/RobeeF/InverseCarbonBudgetEstim>

## 788 **Author contribution**

789 The idea was conceived by CB, CT and JCP. Sampling and experiments onboard PEACETIME  
790 cruise were conducted by CT and MG. The data processing of PAP DY032 data was conducted  
791 by CB with advices from FLM, and the one from PEACETIME data by CB and MG. RF  
792 designed the inversion detection methodology and performed the estimation with advices from  
793 LM. CB and RF led the writing with significant contributions from all authors.

794

## 795 **Acknowledgement**

796 We thank the crew and officers of the R.R.S. DISCOVERY (NERC) for their help during the  
797 PAP DY032 cruise and of the N/O Pourquoi Pas? during the PEACETIME cruise. This study  
798 is a contribution to the PEACETIME project (MISTRALS CNRS INSU, doi:  
799 10.17600/17000300) managed by Cécile Guieu (LOV) and Karine Desboeufs (LISA). We  
800 warmly thank F. Van Wambeke, S. Guasco and B. Zancker for onboard works (enzymatic

801 activities, sugar and amino acids concentrations measurements) during PEACETIME cruise.  
802 We wish to express our gratitude to F. Van Wambeke, S. Giering, T. Anderson and A. Belcher  
803 for stimulating and informative discussions. This manuscript is a contribution of the APERO  
804 project funded by the National Research Agency under the grant APERO [grant number ANR  
805 ANR-21-CE01-0027] and by the French LEFE-Cyber program.

## 806 **Competing interests**

807 The authors declare that they have no conflict of interest.

## 808 **References**

- 809 Alldredge, A. L., and M. W. Silver. 1988. Characteristics, dynamics and significance of  
810 marine snow. *Progress in Oceanography* **20**: 41–82. doi:10.1016/0079-  
811 6611(88)90053-5
- 812 Anderson, T. R., and V. A. Ryabchenko. 2009. Carbon cycling in the Mesopelagic Zone of  
813 the central Arabian Sea: Results from a simple model. Washington DC American  
814 Geophysical Union Geophysical Monograph Series **185**: 281–297.  
815 doi:10.1029/2007GM000686
- 816 Anderson, T. R., and K. W. Tang. 2010. Carbon cycling and POC turnover in the  
817 mesopelagic zone of the ocean: Insights from a simple model. *Deep Sea Research*  
818 *Part II: Topical Studies in Oceanography* **57**: 1581–1592.  
819 doi:10.1016/j.dsr2.2010.02.024
- 820 Arístegui, J., C. M. Duarte, J. M. Gasol, and L. Alonso-Sáez. 2005. Active mesopelagic  
821 prokaryotes support high respiration in the subtropical northeast Atlantic Ocean.  
822 *Geophysical Research Letters* **32**: 1–4. doi:10.1029/2004GL021863
- 823 Arístegui, J., J. M. Gasol, C. M. Duarte, and G. J. Herndl. 2009. Microbial oceanography of  
824 the dark ocean's pelagic realm. *Limnology and Oceanography* **54**: 1501–1529.  
825 doi:10.4319/lo.2009.54.5.1501
- 826 Armstrong, R. A., C. Lee, J. I. Hedges, S. Honjo, and S. G. Wakeham. 2002. A new,  
827 mechanistic model for organic carbon fluxes in the ocean based on the quantitative

828 association of POC with ballast minerals. *Deep Sea Research Part II: Topical Studies*  
829 *in Oceanography* **49**: 219–236. doi:10.1016/S0967-0645(01)00101-1

830 Baltar, F., J. Arístegui, J. M. Gasol, E. Sintes, and G. J. Herndl. 2009. Evidence of  
831 prokaryotic metabolism on suspended particulate organic matter in the dark waters of  
832 the subtropical North Atlantic. *Limnology and Oceanography* **54**: 182–193.  
833 doi:10.4319/lo.2009.54.1.0182

834 Baltar, F., J. Arístegui, E. Sintes, J. M. Gasol, T. Reinthaler, and G. J. Herndl. 2010.  
835 Significance of non-sinking particulate organic carbon and dark CO<sub>2</sub> fixation to  
836 heterotrophic carbon demand in the mesopelagic northeast Atlantic. *Geophysical*  
837 *Research Letters* **37**: n/a-n/a. doi:10.1029/2010GL043105

838 Baumas, C. M. J., F. A. C. Le Moigne, M. Garel, and others. 2021. Mesopelagic microbial  
839 carbon production correlates with diversity across different marine particle fractions.  
840 *The ISME Journal* **15**: 1695–1708. doi:10.1038/s41396-020-00880-z

841 Belcher, A., M. Iversen, S. Giering, V. Riou, S. A. Henson, L. Berline, L. Guilloux, and R.  
842 Sanders. 2016. Depth-resolved particle-associated microbial respiration in the  
843 northeast Atlantic. *Biogeosciences* **13**: 4927–4943. doi:10.5194/bg-13-4927-2016

844 Bochdansky, A. B., M. A. Clouse, and G. J. Herndl. 2017. Eukaryotic microbes, principally  
845 fungi and labyrinthulomycetes, dominate biomass on bathypelagic marine snow. *The*  
846 *ISME Journal* **11**: 362–373. doi:10.1038/ismej.2016.113

847 Bogatyreva, N. S., A. V. Finkelstein, and O. V. Galzitskaya. 2006. Trend of amino acid  
848 composition of proteins of different taxa. *J. Bioinform. Comput. Biol.* **04**: 597–608.  
849 doi:10.1142/S0219720006002016

850 Boyd, P. W., H. Claustre, M. Levy, D. A. Siegel, and T. Weber. 2019. Multi-faceted particle  
851 pumps drive carbon sequestration in the ocean. *Nature*. doi:10.1038/s41586-019-  
852 1098-2

853 Boyd, P. W., A. McDonnell, J. Valdez, D. LeFevre, and M. P. Gall. 2015. RESPIRE: An in  
854 situ particle interceptor to conduct particle remineralization and microbial dynamics

855 studies in the oceans' Twilight Zone. *Limnology and Oceanography: Methods* **13**:  
856 494–508. doi:10.1002/lom3.10043

857 Briggs, N. T., W. H. Slade, E. Boss, and M. J. Perry. 2013. Method for estimating mean  
858 particle size from high-frequency fluctuations in beam attenuation or scattering  
859 measurements. *Appl. Opt.*, AO **52**: 6710–6725. doi:10.1364/AO.52.006710

860 Burd, A. B., D. A. Hansell, D. K. Steinberg, and others. 2010. Assessing the apparent  
861 imbalance between geochemical and biochemical indicators of meso- and  
862 bathypelagic biological activity: What the @\$#! is wrong with present calculations of  
863 carbon budgets? *Deep-Sea Research Part II: Topical Studies in Oceanography*  
864 1557–1571. doi:10.1016/j.dsr2.2010.02.022

865 Carlson, C. A., S. J. Giovannoni, D. A. Hansell, S. J. Goldberg, R. Parsons, and K. Vergin.  
866 2004. Interactions among dissolved organic carbon, microbial processes, and  
867 community structure in the mesopelagic zone of the northwestern Sargasso Sea.  
868 *Limnol. Oceanogr.* **49**: 1073–1083. doi:10.4319/lo.2004.49.4.1073

869 Chang, K. J. L., C. M. Nichols, S. I. Blackburn, G. A. Dunstan, A. Koutoulis, and P. D.  
870 Nichols. 2014. Comparison of *Thraustochytrids* *Aurantiochytrium* sp., *Schizochytrium*  
871 sp., *Thraustochytrium* sp., and *Ulkenia* sp. for Production of Biodiesel, Long-Chain  
872 Omega-3 Oils, and Exopolysaccharide. *Mar Biotechnol* 16.

873 Cho, B. C., and F. Azam. 1988. Major role of bacteria in biogeochemical fluxes in the  
874 ocean's interior. *Nature* **332**: 441–443. doi:10.1038/332441a0

875 Cole, H., S. Henson, A. Martin, and A. Yool. 2012. Mind the gap: The impact of missing data  
876 on the calculation of phytoplankton phenology metrics. *Journal of Geophysical*  
877 *Research: Oceans* **117**. doi:10.1029/2012JC008249

878 Collins, J. R., B. R. Edwards, K. Thamatrakoln, J. E. Ossolinski, G. R. DiTullio, K. D. Bidle,  
879 S. C. Doney, and B. A. S. Van Mooy. 2015. The multiple fates of sinking particles in  
880 the North Atlantic Ocean. *Global Biogeochemical Cycles* **29**: 1471–1494.  
881 doi:10.1002/2014GB005037

882 Cowen, J. P., M. A. Bertram, S. G. Wakeham, R. E. Thomson, J. William Lavelle, E. T.  
883 Baker, and R. A. Feely. 2001. Ascending and descending particle flux from  
884 hydrothermal plumes at Endeavour Segment, Juan de Fuca Ridge. *Deep Sea*  
885 *Research Part I: Oceanographic Research Papers* **48**: 1093–1120.  
886 doi:10.1016/S0967-0637(00)00070-4

887 Dong, S., A. V. Subhas, N. E. Rollins, J. D. Naviaux, J. F. Adkins, and W. M. Berelson. 2018.  
888 A kinetic pressure effect on calcite dissolution in seawater. *Geochimica et*  
889 *Cosmochimica Acta* **238**: 411–423. doi:10.1016/j.gca.2018.07.015

890 Edgcomb, V. P., C. Taylor, M. G. Pachiadaki, S. Honjo, I. Engstrom, and M. Yakimov. 2016.  
891 Comparison of Niskin vs. in situ approaches for analysis of gene expression in deep  
892 Mediterranean Sea water samples. *Deep Sea Research Part II: Topical Studies in*  
893 *Oceanography* **129**: 213–222. doi:10.1016/j.dsr2.2014.10.020

894 Eppley, R. W., and B. J. Peterson. 1979. Particulate organic matter flux and planktonic new  
895 production in the deep ocean. *Nature* **282**: 677–680. doi:10.1038/282677a0

896 Fennel, K., J. P. Mattern, S. C. Doney, L. Bopp, A. M. Moore, B. Wang, and L. Yu. 2022.  
897 Ocean biogeochemical modelling. *Nat Rev Methods Primers* **2**: 1–21.  
898 doi:10.1038/s43586-022-00154-2

899 Fuchs, R., C. M. J. Baumas, M. Garel, D. Nerini, F. A. C. Le Moigne, and C. Tamburini.  
900 2022. A RUpture-Based detection method for the Active mesopeLagic Zone  
901 (RUBALIZ): A crucial step toward rigorous carbon budget assessments. *Limnology*  
902 *and Oceanography: Methods* **n/a**. doi:10.1002/lom3.10520

903 Fuhrman, J. 2000. Impact of Viruses on Bacterial Processes, *In* *Microbial ecology of the*  
904 *oceans*. Wiley.

905 Garel, M., P. Bonin, S. Martini, S. Guasco, M. Roumagnac, N. Bhairy, F. Armougom, and C.  
906 Tamburini. 2019. Pressure-Retaining Sampler and High-Pressure Systems to Study  
907 Deep-Sea Microbes Under In Situ Conditions. *Frontiers in Microbiology* **10**: 453.  
908 doi:10.3389/FMICB.2019.00453

909 Giering, S. L. C., E. L. Cavan, S. L. Basedow, and others. 2020. Sinking Organic Particles in  
910 the Ocean—Flux Estimates From in situ Optical Devices. *Frontiers in Marine Science*  
911 **6**. doi:10.3389/fmars.2019.00834

912 Giering, S. L. C., and C. Evans. 2022. Overestimation of prokaryotic production by leucine  
913 incorporation—and how to avoid it. *Limnology and Oceanography* **1**–13.  
914 doi:10.1002/lno.12032

915 Giering, S. L. C., R. Sanders, R. S. Lampitt, and others. 2014. Reconciliation of the carbon  
916 budget in the ocean’s twilight zone. *Nature* **507**: 480–483. doi:10.1038/nature13123

917 Giering, S. L. C., R. Sanders, A. P. Martin, S. A. Henson, J. S. Riley, C. M. Marsay, and D.  
918 G. Johns. 2017. Particle flux in the oceans: Challenging the steady state assumption.  
919 *Global Biogeochemical Cycles* **31**. doi:10.1002/2016GB005424

920 del Giorgio, P. A., and J. J. Cole. 1998. BACTERIAL GROWTH EFFICIENCY IN NATURAL  
921 AQUATIC SYSTEMS. *Annual Review of Ecology and Systematics* **29**: 503–541.  
922 doi:10.1146/annurev.ecolsys.29.1.503

923 Grossart, H. P., and G. Gust. 2009. Hydrostatic pressure affects physiology and community  
924 structure of marine bacteria during settling to 4000 m: An experimental approach.  
925 *Marine Ecology Progress Series* **390**: 97–104. doi:10.3354/meps08201

926 Grossart, H.-P., and H. Ploug. 2000. Bacterial production and growth efficiencies: Direct  
927 measurements on riverine aggregates. *Limnology and Oceanography* **45**: 436–445.  
928 doi:10.4319/lo.2000.45.2.0436

929 Grossart, H.-P., and H. Ploug. 2001. Microbial degradation of organic carbon and nitrogen  
930 on diatom aggregates. *Limnol. Oceanogr.* **46**: 267–277.  
931 doi:10.4319/lo.2001.46.2.0267

932 Guieu, C., K. Desboeufs, S. Albani, and others. 2020. BIOGEOCHEMICAL dataset collected  
933 during the PEACETIME cruise. doi:https://doi.org/10.17882/75747

934 Hamamoto, Y., and D. Honda. 2019. Nutritional intake of *Aplanochytrium* (*Labyrinthulea*,  
935 *Stramenopiles*) from living diatoms revealed by culture experiments suggesting the

936 new prey–predator interactions in the grazing food web of the marine ecosystem A.  
937 lanora [ed.]. PLoS ONE **14**: e0208941. doi:10.1371/journal.pone.0208941

938 Henson, S. A., R. Sanders, E. Madsen, P. J. Morris, F. Le Moigne, and G. D. Quartly. 2011.  
939 A reduced estimate of the strength of the ocean’s biological carbon pump.  
940 Geophysical Research Letters **38**: n/a-n/a. doi:10.1029/2011GL046735

941 Herndl, G. J., T. Reinthaler, E. Teira, H. van Aken, C. Veth, A. Pernthaler, and J. Pernthaler.  
942 2005. Contribution of *Archaea* to Total Prokaryotic Production in the Deep Atlantic  
943 Ocean. Appl Environ Microbiol **71**: 2303–2309. doi:10.1128/AEM.71.5.2303-  
944 2309.2005

945 Herndl, G., and T. Reinthaler. 2013. Microbial control of the dark end of the biological pump.  
946 Nature Geoscience **6**: 718–724. doi:10.1038/ngeo1921

947 Homma, T., and A. Saltelli. 1996. Importance measures in global sensitivity analysis of  
948 nonlinear models. Reliability Engineering & System Safety **52**: 1–17.  
949 doi:10.1016/0951-8320(96)00002-6

950 Hoppe, H., and S. Ullrich. 1999. Profiles of ectoenzymes in the Indian Ocean: phenomena of  
951 phosphatase activity in the mesopelagic zone. Aquat. Microb. Ecol. **19**: 139–148.  
952 doi:10.3354/ame019139

953 Iversen, M. H., N. Nowald, H. Ploug, G. A. Jackson, and G. Fischer. 2010. High resolution  
954 profiles of vertical particulate organic matter export off Cape Blanc, Mauritania:  
955 Degradation processes and ballasting effects. Deep Sea Research Part I:  
956 Oceanographic Research Papers **57**: 771–784. doi:10.1016/j.dsr.2010.03.007

957 Jain, R., S. Raghukumar, R. Tharanathan, and N. B. Bhosle. 2005. Extracellular  
958 Polysaccharide Production by Thraustochytrid Protists. Mar Biotechnol **7**: 184–192.  
959 doi:10.1007/s10126-004-4025-x

960 Jannasch, H. W., and C. D. Taylor. 1984. Deep-Sea Microbiology. Annual Review of  
961 Microbiology **38**: 487–487. doi:10.1146/annurev.mi.38.100184.002415

962 de Jesus Mendes, P. A., L. Thomsen, B. Holscher, H. C. de Stigter, and G. Gust. 2007.  
963 Pressure effects on the biological degradation of organo-mineral aggregates in



964 submarine canyons. *Marine Geology* **246**: 165–175.  
965 doi:10.1016/j.margeo.2007.05.012

966 Kjørboe, T. 2003. Marine snow microbial communities: scaling of abundances with  
967 aggregate size. *Aquatic Microbial Ecology* **33**: 67–75. doi:10.3354/ame033067

968 Kjørboe, T., H.-P. Grossart, H. Ploug, and K. Tang. 2002. Mechanisms and Rates of  
969 Bacterial Colonization of Sinking Aggregates. *Applied and Environmental*  
970 *Microbiology* **68**: 3996–4006. doi:10.1128/AEM.68.8.3996-4006.2002

971 Kjørboe, T., K. Tang, H.-P. Grossart, and H. Ploug. 2003. Dynamics of Microbial  
972 Communities on Marine Snow Aggregates: Colonization, Growth, Detachment, and  
973 Grazing Mortality of Attached Bacteria. *Applied and Environmental Microbiology* **69**:  
974 3036–3047. doi:10.1128/AEM.69.6.3036-3047.2003

975 Kirchman, D., E. K'nees, and R. Hodson. 1985. Leucine incorporation and its potential as a  
976 measure of protein synthesis by bacteria in natural aquatic systems. *Applied and*  
977 *Environmental Microbiology* **49**: 599–607. doi:10.1128/aem.49.3.599-607.1985

978 Kirchman, D. L., and H. W. Ducklow. 1993. Estimating Conversion Factors for the Thymidine  
979 and Leucine Methods for Measuring Bacterial Production, *In Handbook of Methods in*  
980 *Aquatic Microbial Ecology*. Lewis publishers.

981 Koski, M., B. Valencia, R. Newstead, and C. Thiele. 2020. The missing piece of the upper  
982 mesopelagic carbon budget? Biomass, vertical distribution and feeding of aggregate-  
983 associated copepods at the PAP site. *Progress in Oceanography* **181**: 102243.  
984 doi:10.1016/j.pocean.2019.102243

985 Kuhlisch, C., G. Schleyer, N. Shahaf, F. Vincent, D. Schatz, and A. Vardi. 2021. Viral  
986 infection of algal blooms leaves a unique metabolic footprint on the dissolved organic  
987 matter in the ocean. *Science Advances* **7**: eabf4680. doi:10.1126/sciadv.abf4680

988 Kwon, E. Y., F. Primeau, and J. L. Sarmiento. 2009. The impact of remineralization depth on  
989 the air–sea carbon balance. *Nature Geosci* **2**: 630–635. doi:10.1038/ngeo612

- 990 Lagarias, J. C., J. A. Reeds, M. H. Wright, and P. E. Wright. 1998. Convergence properties  
991 of the Nelder-Mead simplex method in low dimensions. *SIAM Journal on*  
992 *Optimization* **9**: 112–147. doi:10.1137/S1052623496303470
- 993 Lampitt, R. S., B. Boorman, L. Brown, and others. 2008. Particle export from the euphotic  
994 zone: Estimates using a novel drifting sediment trap, <sup>234</sup>Th and new production.  
995 *Deep Sea Research Part I: Oceanographic Research Papers* **55**: 1484–1502.  
996 doi:10.1016/j.dsr.2008.07.002
- 997 Lara, E., D. Vaqué, E. L. Sà, and others. 2017. Unveiling the role and life strategies of  
998 viruses from the surface to the dark ocean. *Sci. Adv.* **3**: e1602565.  
999 doi:10.1126/sciadv.1602565
- 1000 Le Moigne, F. A. C. 2019. Pathways of organic carbon downward transport by the oceanic  
1001 biological carbon pump. *Frontiers in Marine Sciences* **6**: 1–8.  
1002 doi:10.3389/fmars.2019.00634
- 1003 Le Moigne, F. A. C., S. A. Henson, E. Cavan, and others. 2016. What causes the inverse  
1004 relationship between primary production and export efficiency in the Southern  
1005 Ocean? *Geophysical Research Letters* **43**: 4457–4466. doi:10.1002/2016GL068480
- 1006 Lemée, R., E. Rochelle-Newall, F. Van Wambeke, M. Pizay, P. Rinaldi, and J. Gattuso.  
1007 2002. Seasonal variation of bacterial production, respiration and growth efficiency in  
1008 the open NW Mediterranean Sea. *Aquatic Microbial Ecology* **29**: 227–237.  
1009 doi:10.3354/ame029227
- 1010 Liu, Y., M. Zeng, Z. Xie, D. Ning, J. Zhou, X. Yu, R. Liu, and L. Zhang. 2022. Microbial  
1011 Community Structure and Ecological Networks during Simulation of Diatom Sinking.  
1012 1–20.
- 1013 Luo, E., A. O. Leu, J. M. Eppley, D. M. Karl, and E. F. DeLong. 2022. Diversity and origins of  
1014 bacterial and archaeal viruses on sinking particles reaching the abyssal ocean. *The*  
1015 *ISME Journal* 1–9. doi:10.1038/s41396-022-01202-1
- 1016 Marsay, C. M., R. J. Sanders, S. A. Henson, K. Pabortsava, E. P. Achterberg, and R. S.  
1017 Lampitt. 2015. Attenuation of sinking particulate organic carbon flux through the

1018 mesopelagic ocean. *Proceedings of the National Academy of Sciences* **112**: 1089–  
1019 1094. doi:10.1073/pnas.1415311112

1020 Martin, J. H., G. A. Knauer, D. M. Karl, and W. W. Broenkow. 1987. VERTEX: carbon cycling  
1021 in the northeast Pacific. *Deep Sea Research Part A. Oceanographic Research*  
1022 *Papers* **34**: 267–285. doi:10.1016/0198-0149(87)90086-0

1023 McDonnell, A. M. P., P. J. Lam, C. H. Lamborg, and others. 2015. The oceanographic  
1024 toolbox for the collection of sinking and suspended marine particles. *Progress in*  
1025 *Oceanography* **133**: 17–31. doi:10.1016/j.pocean.2015.01.007

1026 Mendes, P. A. de J., and L. Thomsen. 2012. Effects of Ocean Acidification on the Ballast of  
1027 Surface Aggregates Sinking through the Twilight Zone. *PLOS ONE* **7**: e50865.  
1028 doi:10.1371/journal.pone.0050865

1029 Nagata, T., C. Tamburini, J. Arístegui, and others. 2010. Emerging concepts on microbial  
1030 processes in the bathypelagic ocean – ecology, biogeochemistry, and genomics.  
1031 *Deep Sea Research Part II: Topical Studies in Oceanography* **57**: 1519–1536.  
1032 doi:10.1016/j.dsr2.2010.02.019

1033 Nelder, J. A., and R. Mead. 1965. A Simplex Method for Function Minimization. *The*  
1034 *Computer Journal* **7**: 308–313. doi:10.1093/comjnl/7.4.308

1035 Pedrosa-Pàmies, R., M. H. Conte, J. C. Weber, and R. Johnson. 2019. Hurricanes Enhance  
1036 Labile Carbon Export to the Deep Ocean. *Geophysical Research Letters* **46**: 10484–  
1037 10494. doi:10.1029/2019GL083719

1038 Picheral, M., C. Catalano, D. Brousseau, and others. 2022. THE UNDERWATER VISION  
1039 PROFILER 6: AN IMAGING SENSOR OF PARTICLE SIZE SPECTRA AND PLANKTON, FOR  
1040 AUTONOMOUS AND CABLED PLATFORMS. *Limnology & Ocean Methods* **20**: 115–129.  
1041 doi:10.1002/lom3.10475

1042 Planquette, H., and R. M. Sherrell. 2012. Sampling for particulate trace element  
1043 determination using water sampling bottles: methodology and comparison to in situ  
1044 pumps. *Limnology and Oceanography: Methods* **10**: 367–388.  
1045 doi:10.4319/lom.2012.10.367

1046 Reinthaler, T., H. M. van Aken, and G. J. Herndl. 2010. Major contribution of autotrophy to  
1047 microbial carbon cycling in the deep North Atlantic's interior. *Deep Sea Research*  
1048 *Part II: Topical Studies in Oceanography* **57**: 1572–1580.  
1049 doi:10.1016/j.dsr2.2010.02.023

1050 Reinthaler, T., H. van Aken, C. Veth, J. Arístegui, C. Robinson, P. J. L. B. Williams, P.  
1051 Lebaron, and G. J. Herndl. 2006. Prokaryotic respiration and production in the meso-  
1052 and bathypelagic realm of the eastern and western North Atlantic basin. *Limnology*  
1053 *and Oceanography* **51**: 1262–1273. doi:10.4319/lo.2006.51.3.1262

1054 Riley, J. S., R. Sanders, C. Marsay, F. A. C. Le Moigne, E. P. Achterberg, and A. J. Poulton.  
1055 2012. The relative contribution of fast and slow sinking particles to ocean carbon  
1056 export. *Global Biogeochemical Cycles* **26**: 1–10. doi:10.1029/2011GB004085

1057 Riou, V., J. Para, M. Garel, and others. 2018. Biodegradation of *Emiliania huxleyi*  
1058 aggregates by a natural Mediterranean prokaryotic community under increasing  
1059 hydrostatic pressure. *Progress in Oceanography* **163**: 271–281.  
1060 doi:10.1016/j.pocean.2017.01.005

1061 Robert, A. 2012. Minéralisation in situ de la matière organique le long de la colonne d'eau :  
1062 application sur une station eulérienne. These de doctorat. Aix-Marseille.

1063 Russell, J. B., and G. M. Cook. 1995. Energetics of Bacterial Growth: Balance of Anabolic  
1064 and Catabolic Reactions. *MICROBIOL. REV.* **59**: 15.

1065 Saint-Béat, B., B. D. Fath, C. Aubry, and others. 2020. Contrasting pelagic ecosystem  
1066 functioning in eastern and western Baffin Bay revealed by trophic network modeling.  
1067 *Elementa: Science of the Anthropocene* **8**. doi:10.1525/elementa.397

1068 Saint-Béat, B., F. Maps, and M. Babin. 2018. Unraveling the intricate dynamics of planktonic  
1069 Arctic marine food webs. A sensitivity analysis of a well-documented food web  
1070 model. *Progress in Oceanography* **160**: 167–185. doi:10.1016/j.pocean.2018.01.003

1071 Sherry, N. D., P. W. Boyd, K. Sugimoto, and P. J. Harrison. 1999. Seasonal and spatial  
1072 patterns of heterotrophic bacterial production, respiration, and biomass in the

1073 subarctic NE Pacific. *Deep Sea Research Part II: Topical Studies in Oceanography*  
1074 **46**: 2557–2578. doi:10.1016/S0967-0645(99)00076-4

1075 Siegel, D. A., K. O. Buesseler, M. J. Behrenfeld, and others. 2016. Prediction of the Export  
1076 and Fate of Global Ocean Net Primary Production: The EXPORTS Science Plan.  
1077 *Frontiers in Marine Science* **3**: 22. doi:10.3389/fmars.2016.00022

1078 Simon, M., and F. Azam. 1989. Protein content and protein synthesis rates of planktonic  
1079 marine bacteria. *Marine Ecology Progress Series*. doi:10.3354/meps051201

1080 Smith, D. C., M. Simon, A. L. Alldredge, and F. Azam. 1992. Intense hydrolytic enzyme  
1081 activity on marine aggregates and implications for rapid particle dissolution. *Nature*  
1082 **359**: 139–142. doi:10.1038/359139a0

1083 Smith, K. L., P. M. Williams, and E. R. M. Druffel. 1989. Upward fluxes of particulate organic  
1084 matter in the deep North Pacific. *Nature* **337**: 724–726. doi:10.1038/337724a0

1085 Sobol, M. 1993. *Sensitivity Estimates for Nonlinear Mathematical Models*. 8.

1086 Stange, P., L. T. Bach, F. a. C. Le Moigne, J. Taucher, T. Boxhammer, and U. Riebesell.  
1087 2017. Quantifying the time lag between organic matter production and export in the  
1088 surface ocean: Implications for estimates of export efficiency. *Geophysical Research*  
1089 *Letters* **44**: 268–276. doi:10.1002/2016GL070875

1090 Steinberg, D. K., B. A. S. Van Mooy, K. O. Buesseler, P. W. Boyd, T. Kobari, and D. M. Karl.  
1091 2008. Bacterial vs. zooplankton control of sinking particle flux in the ocean’s twilight  
1092 zone. *Limnology and Oceanography* **53**: 1327–1338. doi:10.4319/lo.2008.53.4.1327

1093 Stief, P., M. Elvert, and R. N. Glud. 2021. Respiration by “marine snow” at high hydrostatic  
1094 pressure: Insights from continuous oxygen measurements in a rotating pressure  
1095 tank. *Limnol Oceanogr* **66**: 2797–2809. doi:10.1002/lno.11791

1096 Tamburini, C., M. Boutrif, M. Garel, R. R. Colwell, and J. D. Deming. 2013. Prokaryotic  
1097 responses to hydrostatic pressure in the ocean—a review. *Environmental*  
1098 *microbiology reports* **15**: 1262–1274.

- 1099 Tamburini, C., J. Garcin, and A. Bianchi. 2003. Role of deep-sea bacteria in organic matter  
1100 mineralization and adaptation to hydrostatic pressure conditions in the NW  
1101 Mediterranean Sea. *Aquatic Microbial Ecology* **32**: 209–218. doi:10.3354/ame032209
- 1102 Tamburini, C., J. Garcin, G. Grégori, K. Leblanc, P. Rimmelin, and D. L. Kirchman. 2006.  
1103 Pressure effects on surface Mediterranean prokaryotes and biogenic silica  
1104 dissolution during a diatom sinking experiment. *Aquatic Microbial Ecology* **43**: 267–  
1105 276. doi:10.3354/ame043267
- 1106 Tamburini, C., J. Garcin, M. Ragot, and A. Bianchi. 2002. Biopolymer hydrolysis and  
1107 bacterial production under ambient hydrostatic pressure through a 2000m water  
1108 column in the NW Mediterranean. *Deep Sea Research Part II: Topical Studies in*  
1109 *Oceanography* **49**: 2109–2123. doi:10.1016/S0967-0645(02)00030-9
- 1110 Tamburini, C., M. Garel, A. Barani, and others. 2021. Increasing Hydrostatic Pressure  
1111 Impacts the Prokaryotic Diversity during *Emiliana huxleyi* Aggregates Degradation.  
1112 *Water* **13**: 2616. doi:10.3390/w13192616
- 1113 Tamburini, C., M. Goutx, C. Guigue, and others. 2009. Effects of hydrostatic pressure on  
1114 microbial alteration of sinking fecal pellets. *Deep Sea Research Part II: Topical*  
1115 *Studies in Oceanography* **56**: 1533–1546. doi:10.1016/j.dsr2.2008.12.035
- 1116 Tarantola, A. 2005. *Inverse Problem Theory and Methods for Model Parameter Estimation*,  
1117 Society for Industrial and Applied Mathematics.
- 1118 Tian, R. C., A. F. Ve, B. Klein, T. Packard, S. Roy, C. Savenko, and N. Silverberg. 2000.  
1119 Effects of pelagic food-web interactions and nutrient remineralization on the  
1120 biogeochemical cycling of carbon: a modeling approach. 26.
- 1121 Trull, T. W., S. G. Bray, K. O. Buesseler, C. H. Lamborg, S. Manganini, C. Moy, and J.  
1122 Valdes. 2008. In situ measurement of mesopelagic particle sinking rates and the  
1123 control of carbon transfer to the ocean interior during the Vertical Flux in the Global  
1124 Ocean (VERTIGO) voyages in the North Pacific. *Deep Sea Research Part II: Topical*  
1125 *Studies in Oceanography* **55**: 1684–1695. doi:10.1016/j.dsr2.2008.04.021

- 1126 Turley, C., and P. Mackie. 1994. Biogeochemical significance of attached and free-living  
1127 bacteria and the flux of particles in the NE Atlantic Ocean. *Marine Ecology Progress*  
1128 *Series* **115**: 191–203. doi:10.3354/meps115191
- 1129 Turner, J. T. 2015. Zooplankton fecal pellets, marine snow, phytodetritus and the ocean's  
1130 biological pump. *Progress in Oceanography* **130**: 205–248.  
1131 doi:10.1016/j.pocean.2014.08.005
- 1132 Vetter, Y. A., J. W. Deming, P. A. Jumars, and B. B. Krieger-Brockett. 1998. A Predictive  
1133 Model of Bacterial Foraging by Means of Freely Released Extracellular Enzymes.  
1134 *Microb Ecol* **36**: 75–92. doi:10.1007/s002489900095
- 1135 Wakeham, S. G., C. Lee, J. I. Hedges, P. J. Hernes, and M. J. Peterson. 1997. Molecular  
1136 indicators of diagenetic status in marine organic matter. *Geochimica et*  
1137 *Cosmochimica Acta* **61**: 5363–5369. doi:10.1016/S0016-7037(97)00312-8
- 1138 Weiss, M. S., U. Abele, J. Weckesser, W. Welte, E. Schiltz, and G. E. Schulz. 1991.  
1139 Molecular architecture and electrostatic properties of a bacterial porin. *Science* **254**:  
1140 1627–1630. doi:10.1126/science.1721242
- 1141 Welch, W. J., M. -j. Gething, A. R. Clarke, and others. 1993. Heat shock proteins functioning  
1142 as molecular chaperones: their roles in normal and stressed cells. *Philosophical*  
1143 *Transactions of the Royal Society of London. Series B: Biological Sciences* **339**:  
1144 327–333. doi:10.1098/rstb.1993.0031
- 1145 Westerhoff, H. V., K. J. Hellingwerf, and K. Van Dam. 1983. Thermodynamic efficiency of  
1146 microbial growth is low but optimal for maximal growth rate. *Proc. Natl. Acad. Sci.*  
1147 *U.S.A.* **80**: 305–309. doi:10.1073/pnas.80.1.305
- 1148 Wilhem, W., and C. A. Suttle. 1999. *Viruses and Nutrient Cycles in the Sea.* **49**: 8.
- 1149 Xie, N., M. Bai, L. Liu, and others. 2022. Patchy Blooms and Multifarious Ecotypes of  
1150 *Labyrinthulomycetes* Protists and Their Implication in Vertical Carbon Export in the  
1151 Pelagic Eastern Indian Ocean A.L. Dos Santos [ed.]. *Microbiol Spectr* **10**: e00144-22.  
1152 doi:10.1128/spectrum.00144-22

- 1153 Yayanos, A. A. 1986. Evolutional and ecological implications of the properties of deep-sea  
1154 barophilic bacteria. Proc. Natl. Acad. Sci. U.S.A. **83**: 9542–9546.  
1155 doi:10.1073/pnas.83.24.9542
- 1156 Young, H. L. 1968. Uptake and Incorporation of Exogenous Leucine in Bacterial Cells under  
1157 High Oxygen Tension. Nature **219**: 1068–1069. doi:10.1038/2191068a0
- 1158